Wireless Communications

Principles and Practice

2nd Edition

T.S. Rappaport

Chapter 5: Mobile Radio Propagation: Small-Scale Fading and Multipath as it applies to Modulation Techniques

Doppler Shift Geomerty

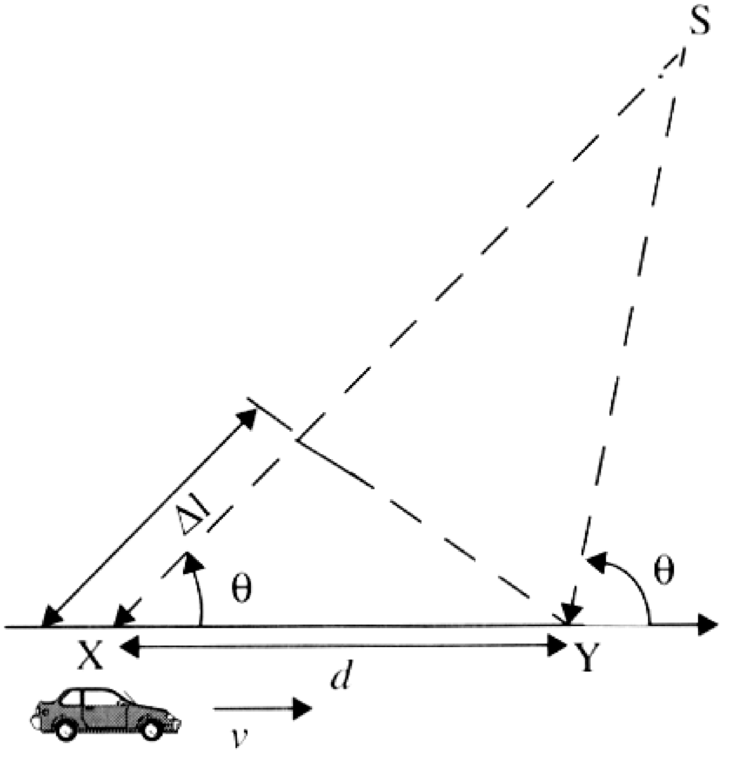

Figure 5.1 Illustration of Doppler effect.

Channel issues

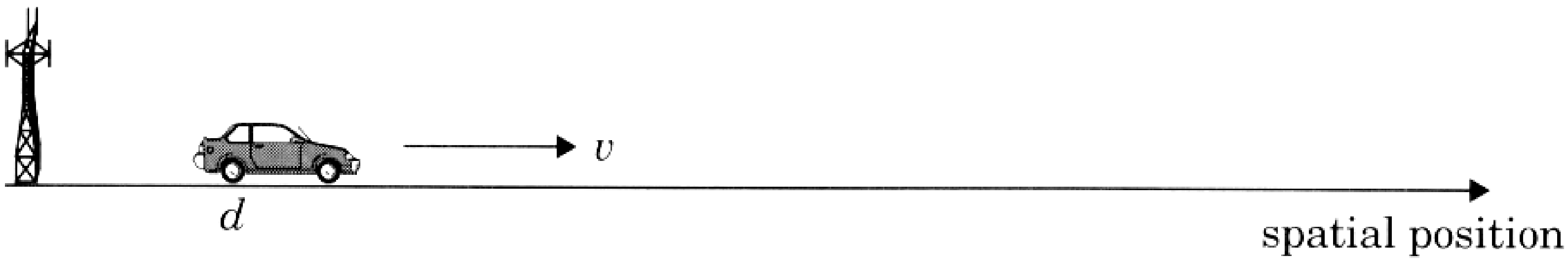

Figure 5.2 The mobile radio channel as a function of time and space.

Complex Baseband model for RF systems

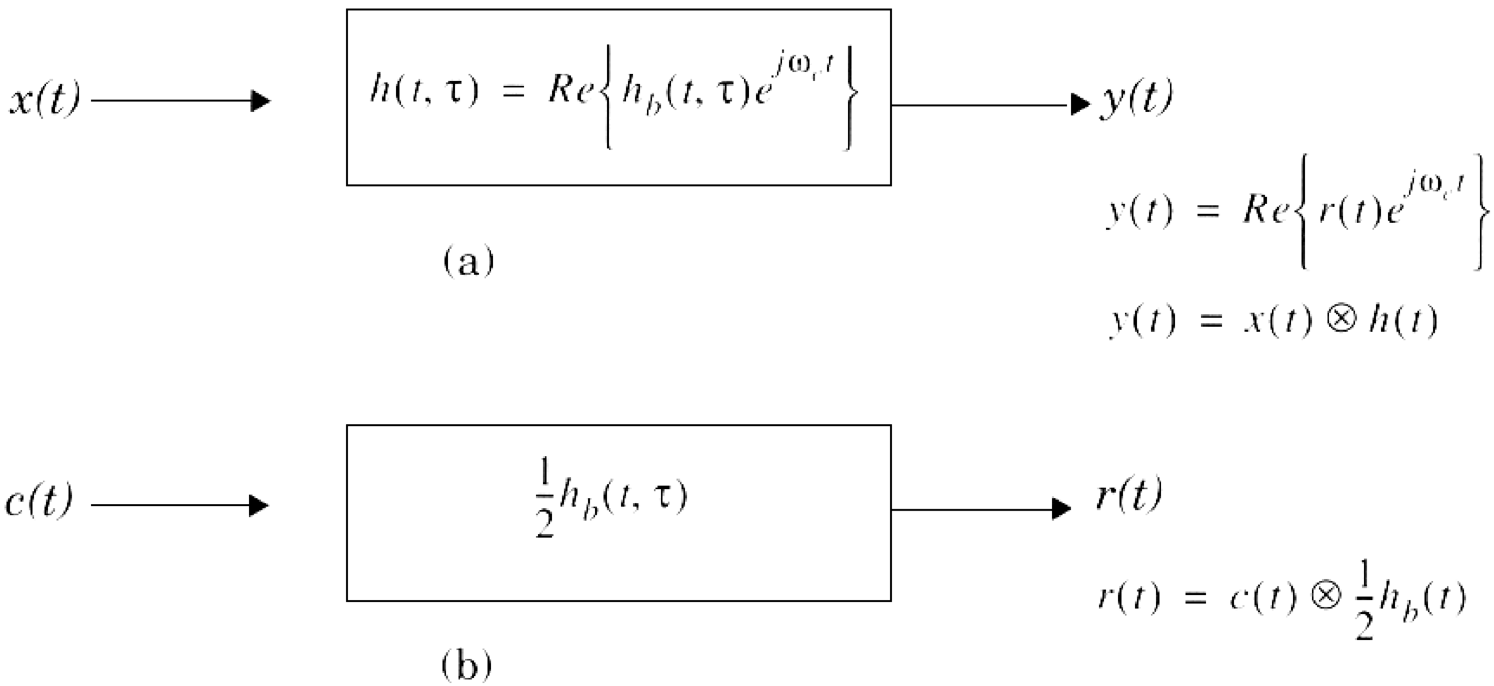

Figure 5.3 (a) Bandpass channel impulse response model; (b) baseband equivalent channel impulse response model.

Time-varying impulse response

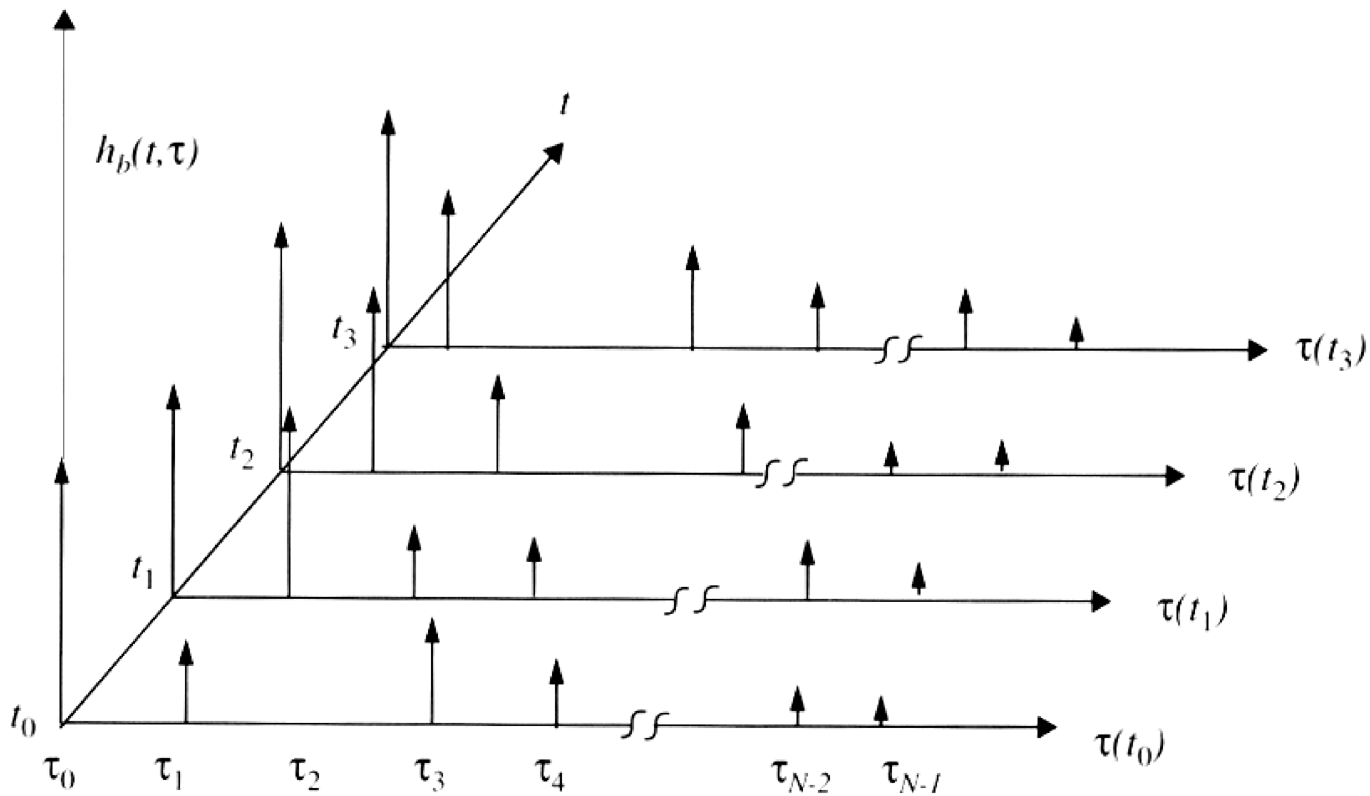

Figure 5.4 An example of the time varying discrete-time impulse response model for a multipath radio channel. Discrete models are useful in simulation where modulation data must be convolved with the channel impulse response [Tra02].

Measured impulse responses

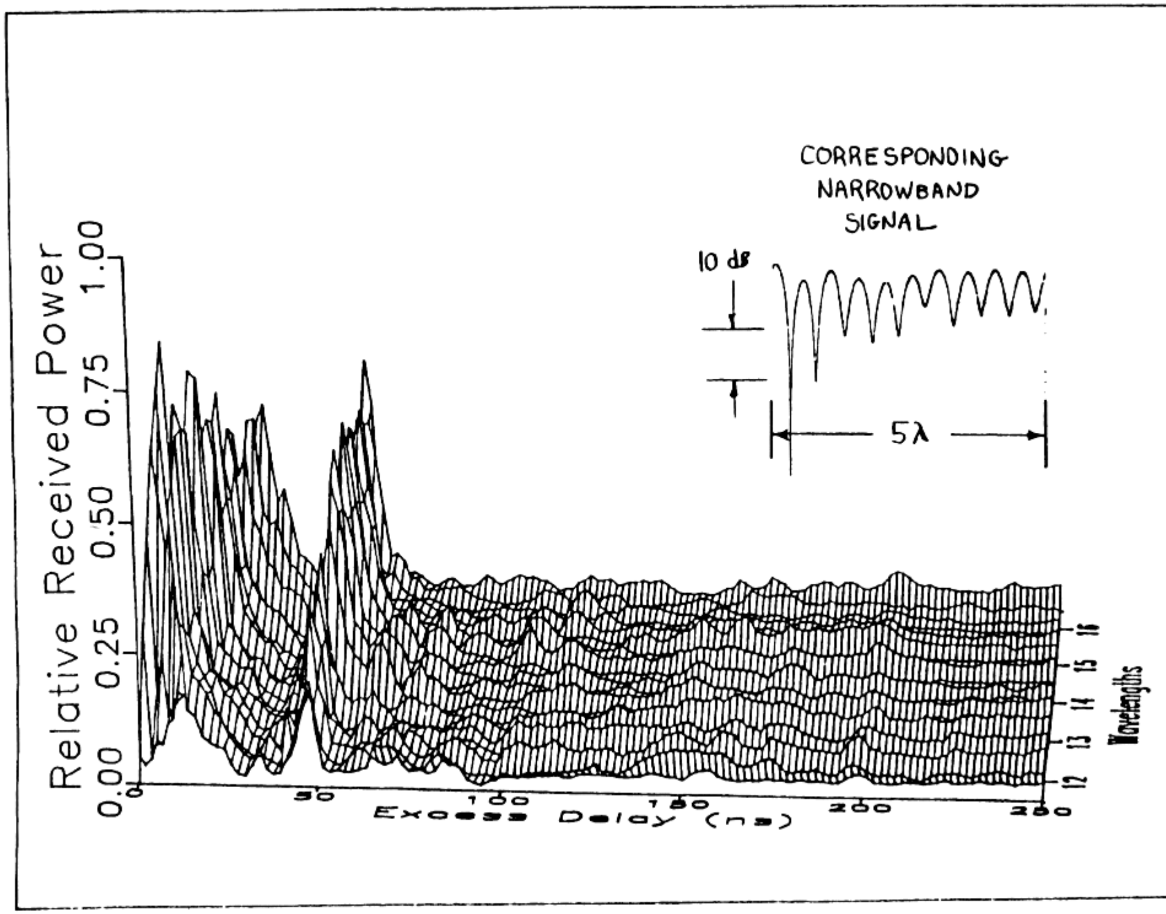

Figure 5.5 Measured wideband and narrowband received signals over a 5λ (0.375 m) measurement track inside a building. Carrier frequency is 4 GHz. Wideband power is computed using Equation (5.19), which can be thought of as the area under the power delay profile. The axis into the page is distance (wavelengths) instead of time.

Channel Sounder: Pulse type

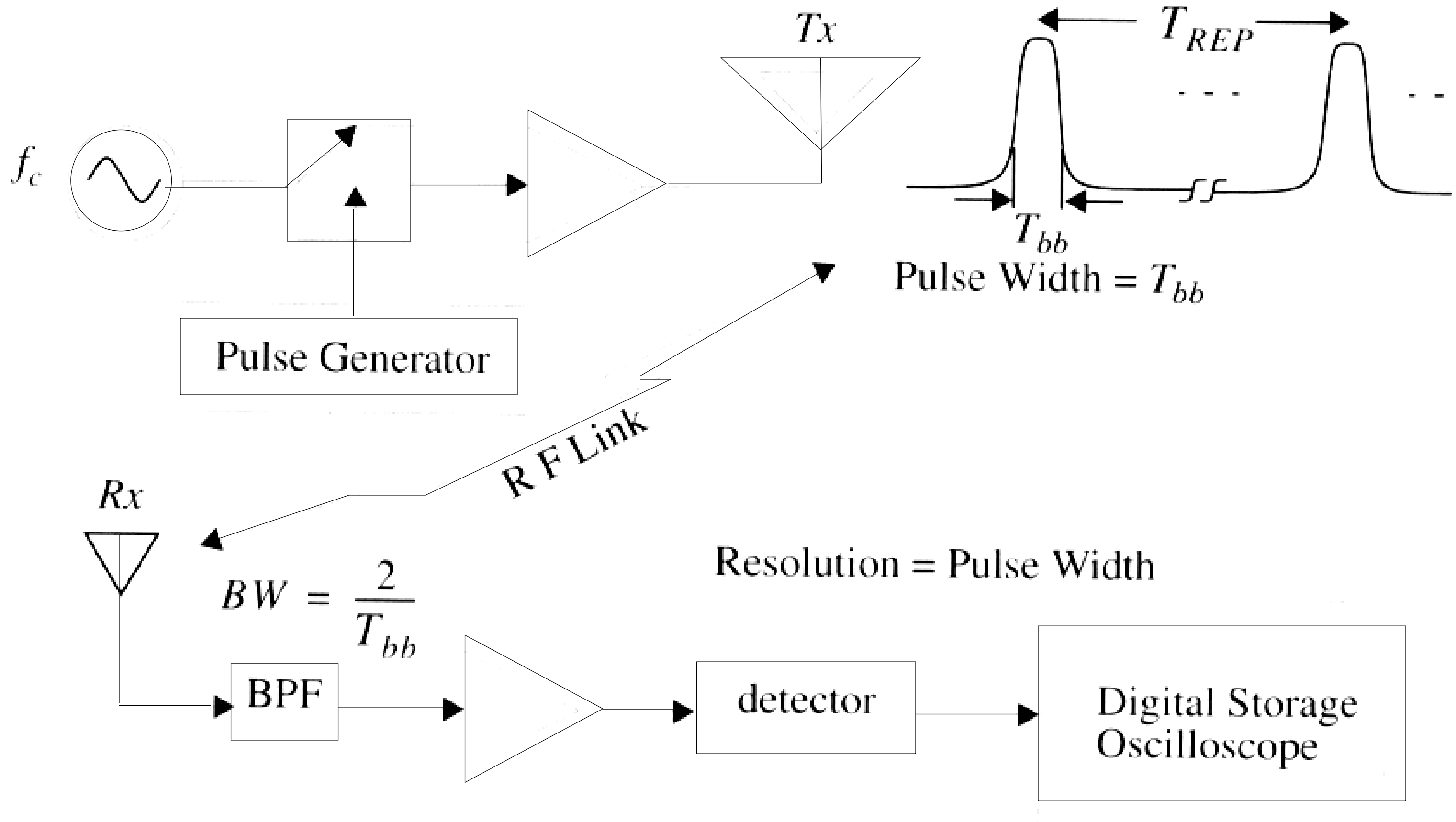

Figure 5.6 Direct RF channel impulse response measurement system.

Channel Sounder: PN Type

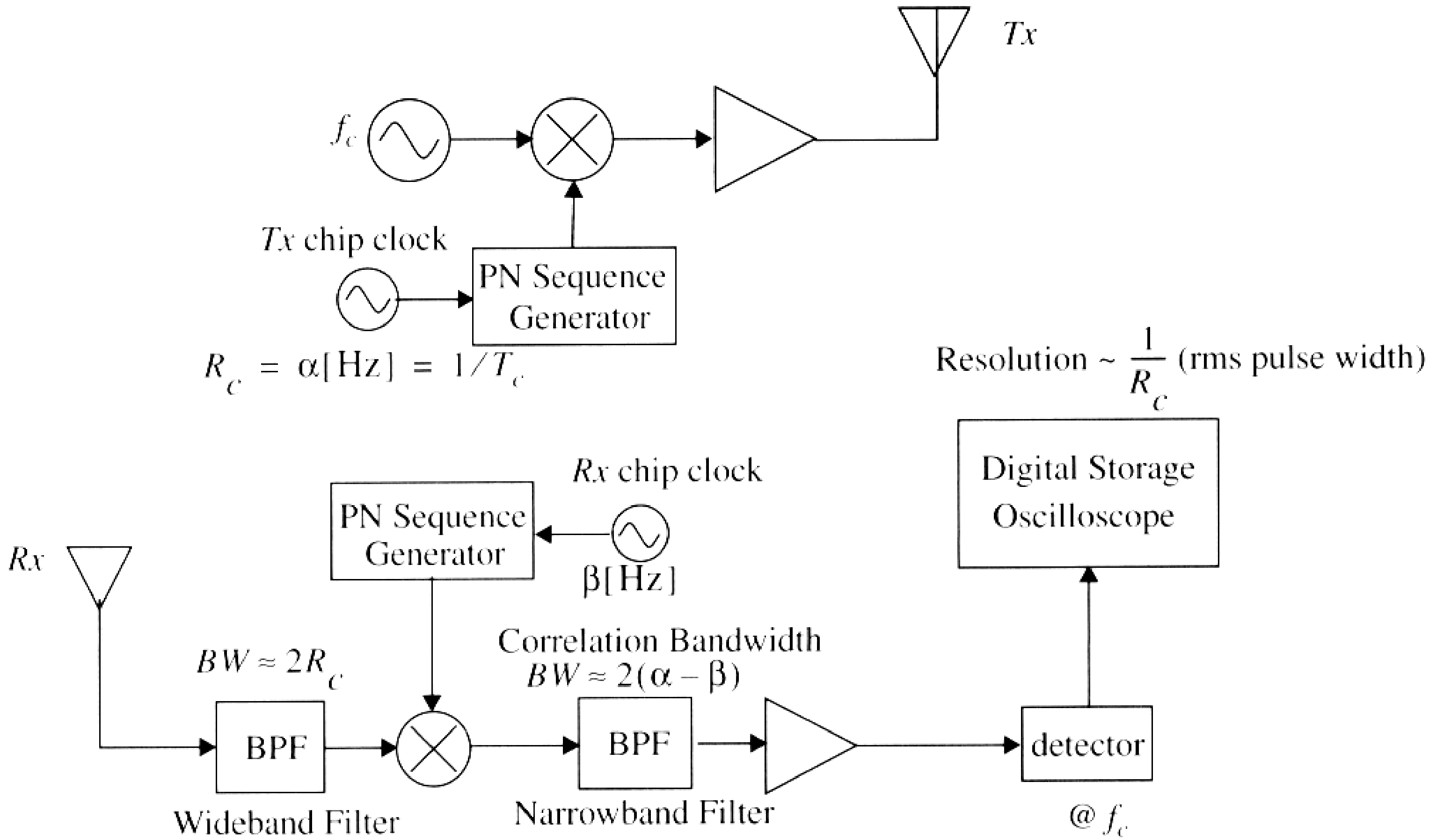

Figure 5.7 Spread spectrum channel impulse response measurement system.

Channel Sounder: Swept Freq. type

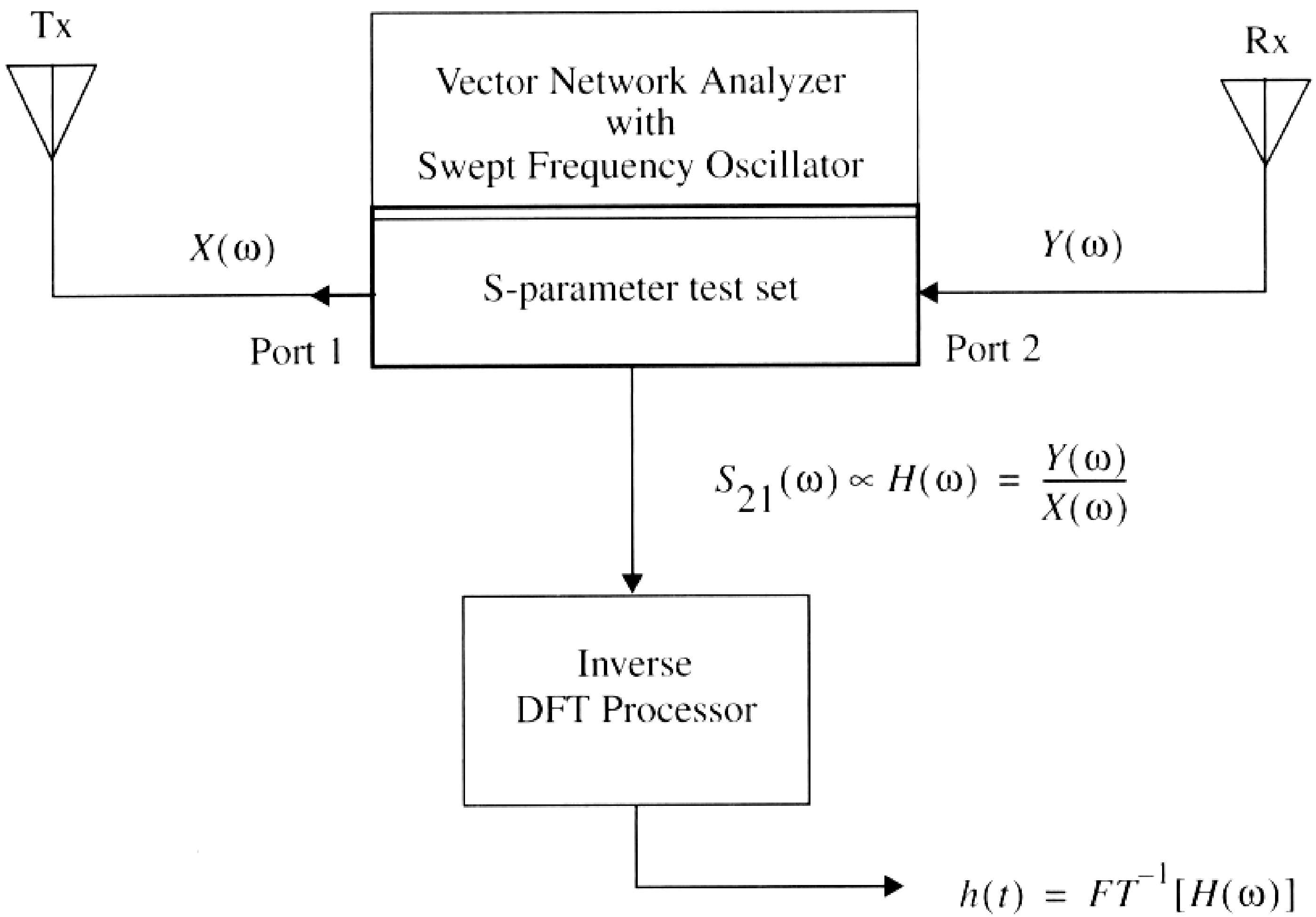

Figure 5.8 Frequency domain channel impulse response measurement system.

Measured power delay profiles

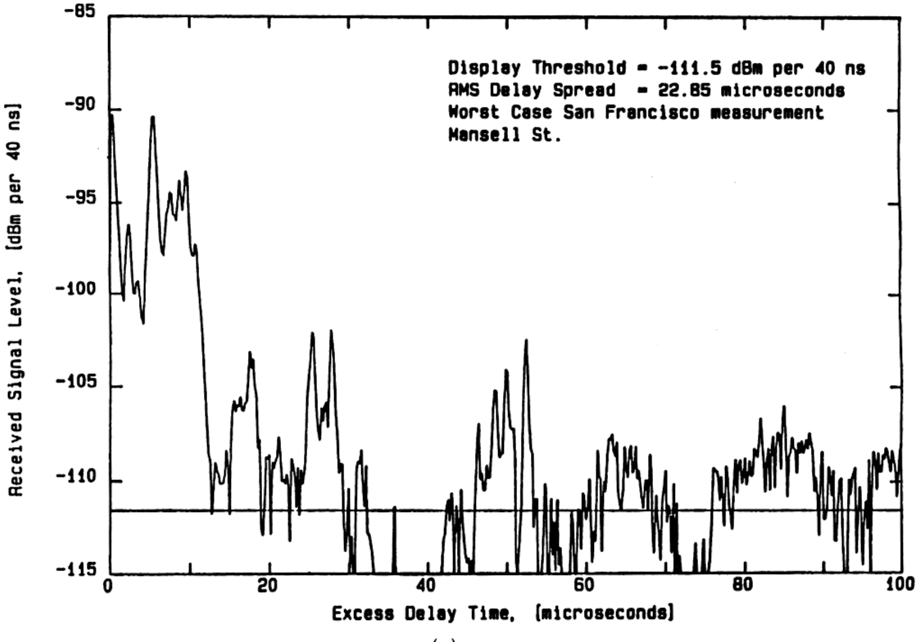

(a)

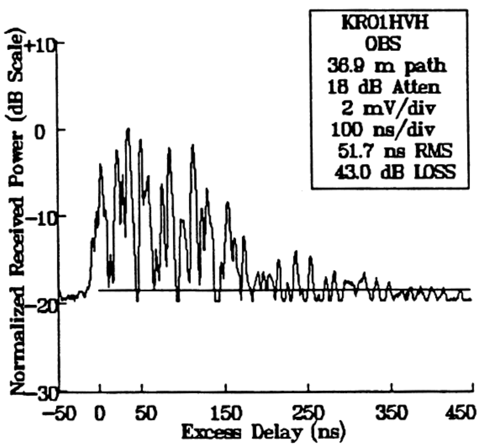

(b)

Figure 5.9 Measured multipath power delay profiles: a) From a 900 MHz cellular system in San Francisco [from [Rap90] © IEEE]; b) inside a grocery store at 4 GHz [from [Haw91] © IEEE].

Indoor Power Delay Profile

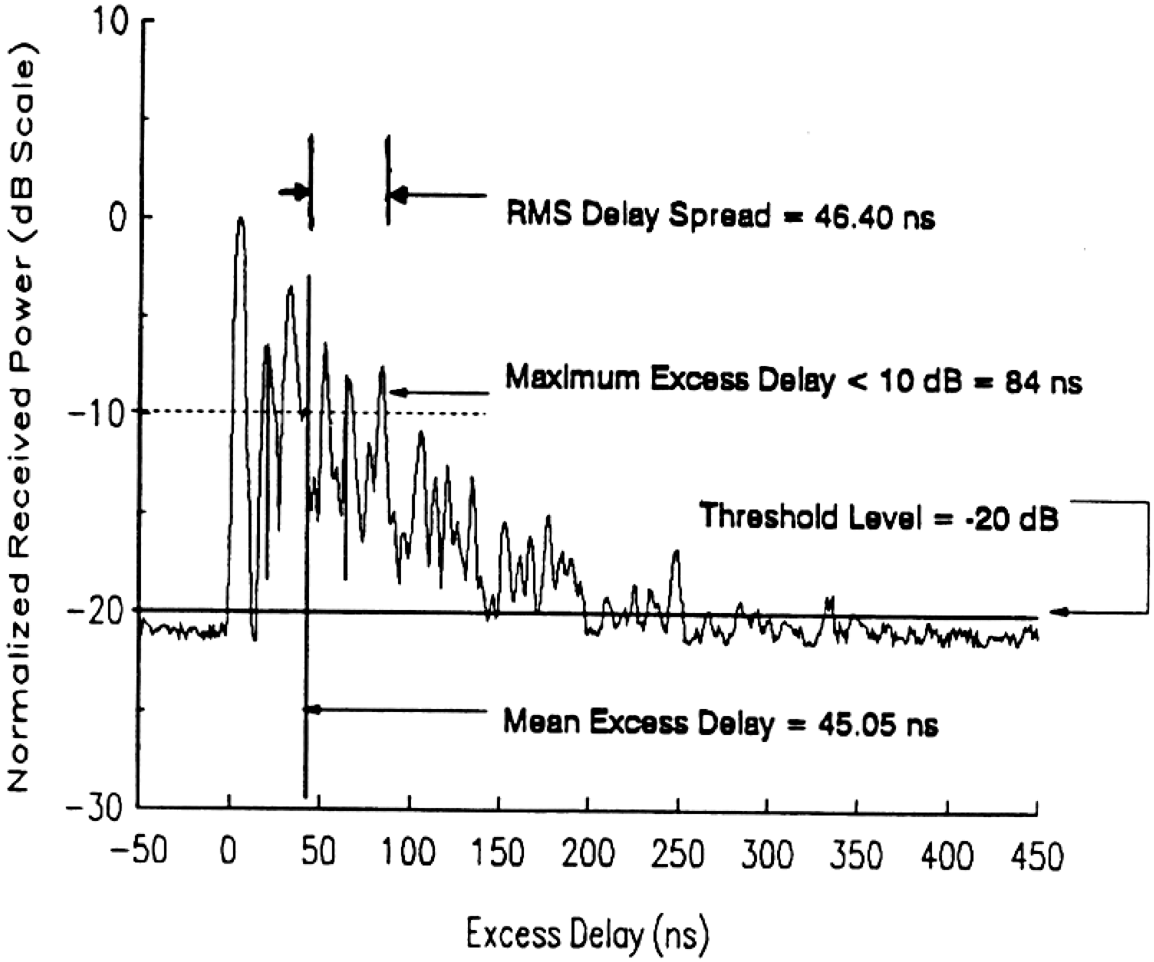

Figure 5.10 Example of an indoor power delay profile; rms delay spread, mean excess delay, maximum excess delay (10 dB), and threshold level are shown.

Typical RMS delay spreads

Table 5.1 Typical Measured Values of RMS Delay Spread

Environment	Frequency (MHz)	RMS Delay Spread (σ_τ)	Notes	Reference
Urban	910	1300 ns avg. 600 ns st. dev. 3500 ns max.	New York City	[Cox75]
Urban	892	10–25 μs	Worst case San Francisco	[Rap90]
Suburban	910	200–310 ns	Averaged typical case	[Cox72]
Suburban	910	1960–2110 ns	Averaged extreme case	[Cox72]
Indoor	1500	10–50 ns 25 ns median	Office building	[Sal87]
Indoor	850	270 ns max.	Office building	[Dev90a]
Indoor	1900	70–94 ns avg. 1470 ns max.	Three San Francisco buildings	[Sei92a]

GSM - TDMA/FDMA

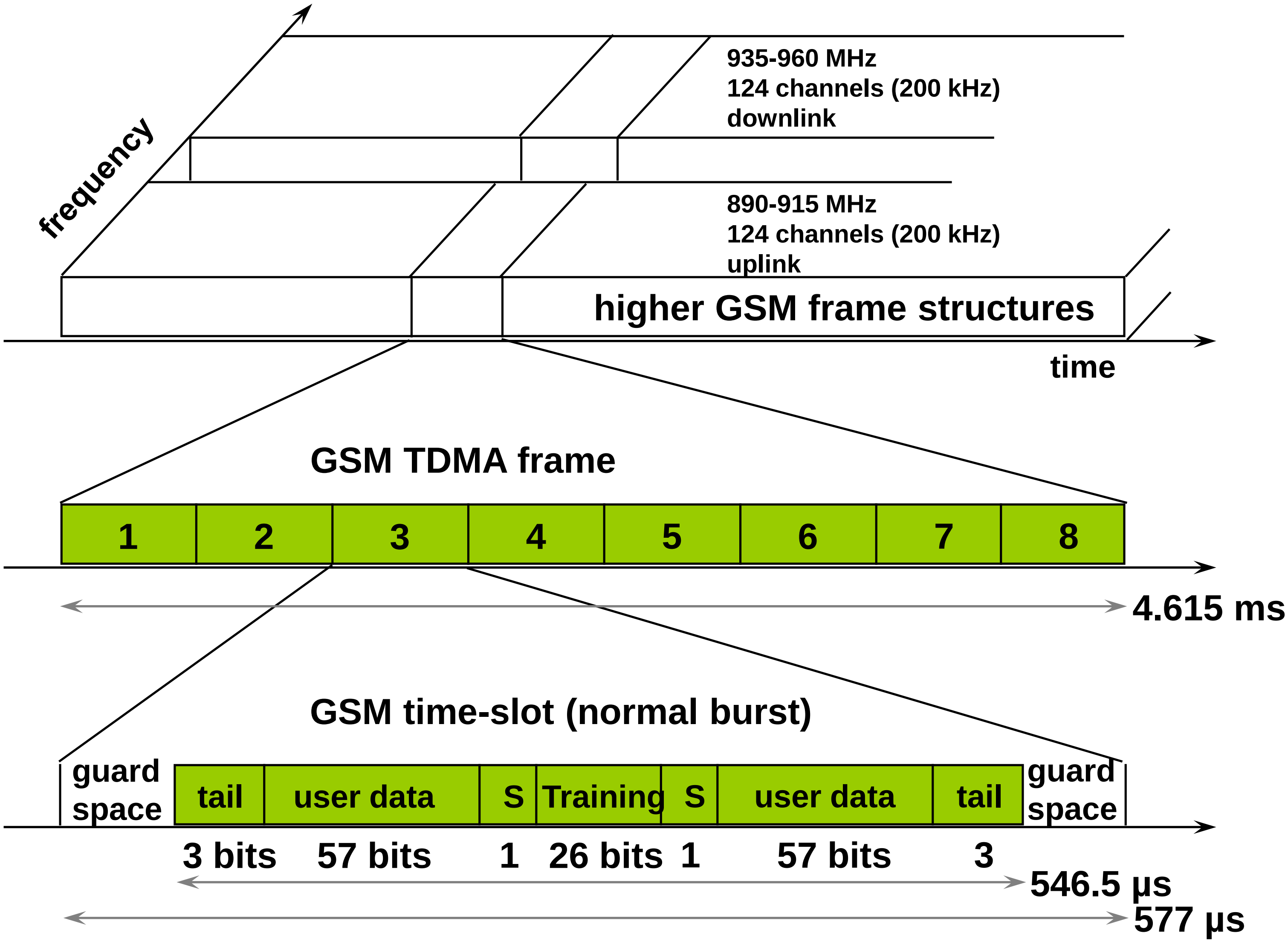

- GSM is designed to support mobile users with a maximum speed of 250 Km/Hour.
- Channel impulse responses are expected to have a max. length of 15 usec (including about 4 bits).

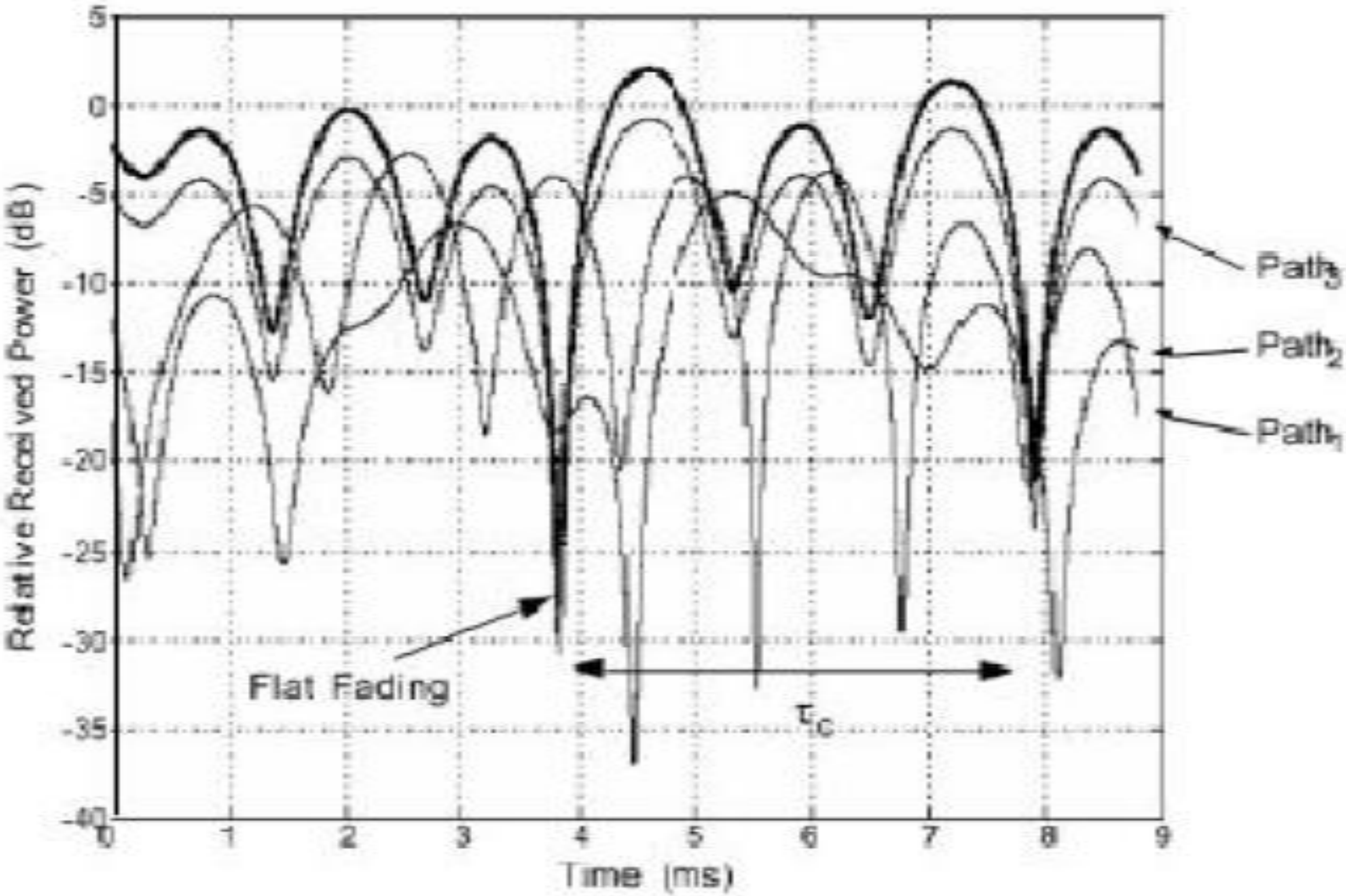

5
0
-5
-10
-15
-20
-25
-30
-35
-40
Relative Received Power (dB)
0
1
2
3
4
5
6
7
8
9
Time (ms)
Path3
Path2
Path1
Flat Fading
τc

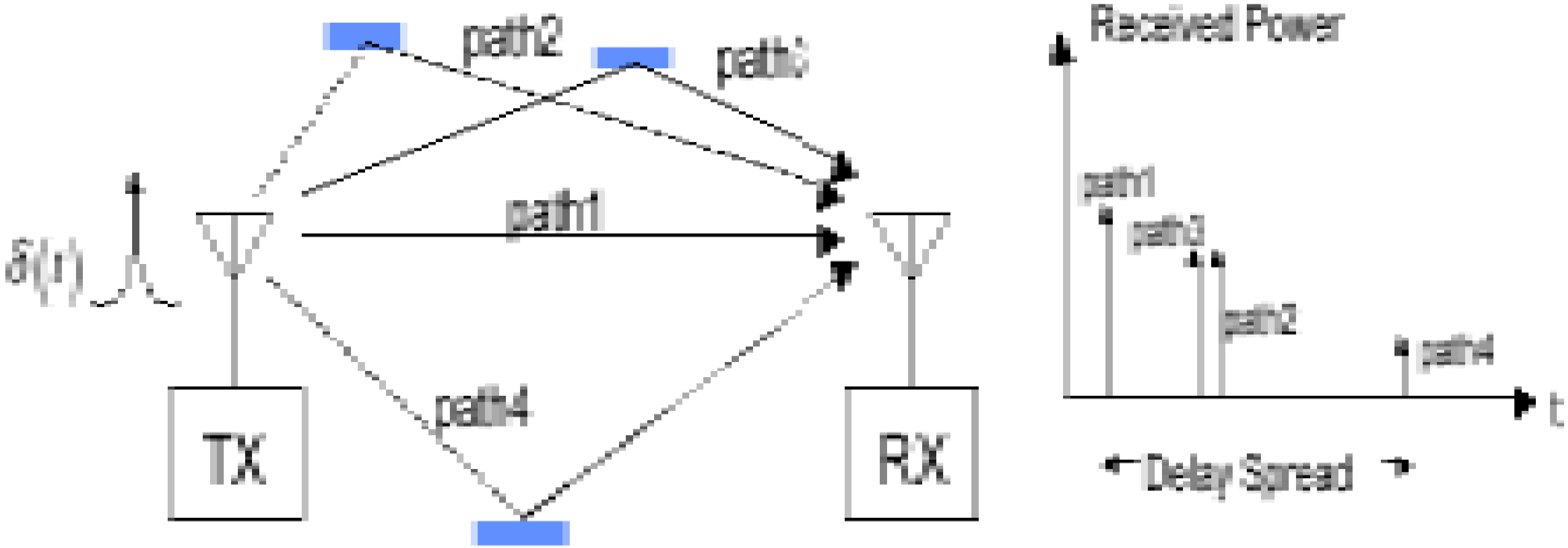
path2
path3
path1
path4
TX
RX
Received Power
path1
path3
path2
path4
t
Delay Spread

Two independent fading issues

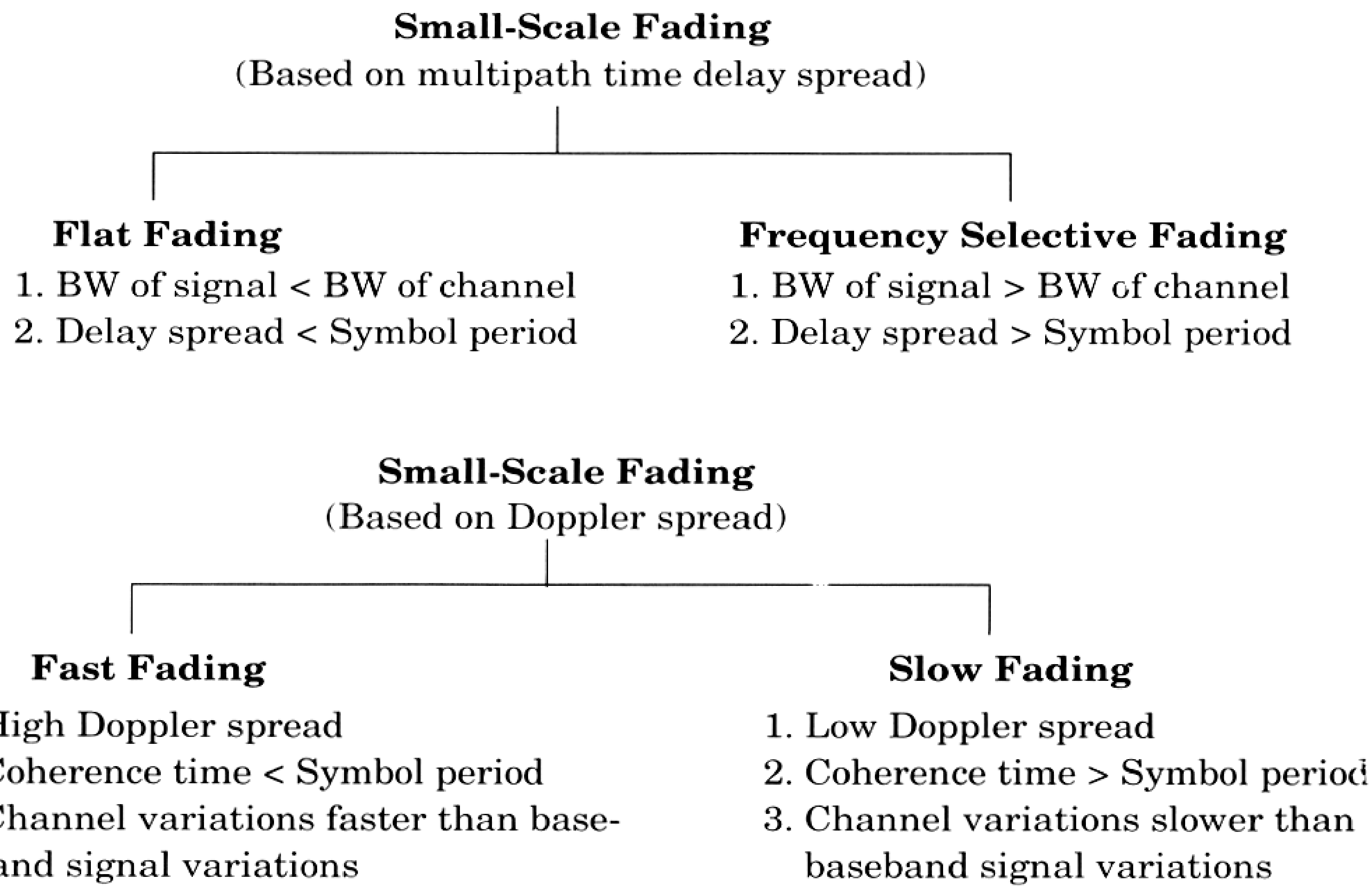

Figure 5.11 Types of small-scale fading.

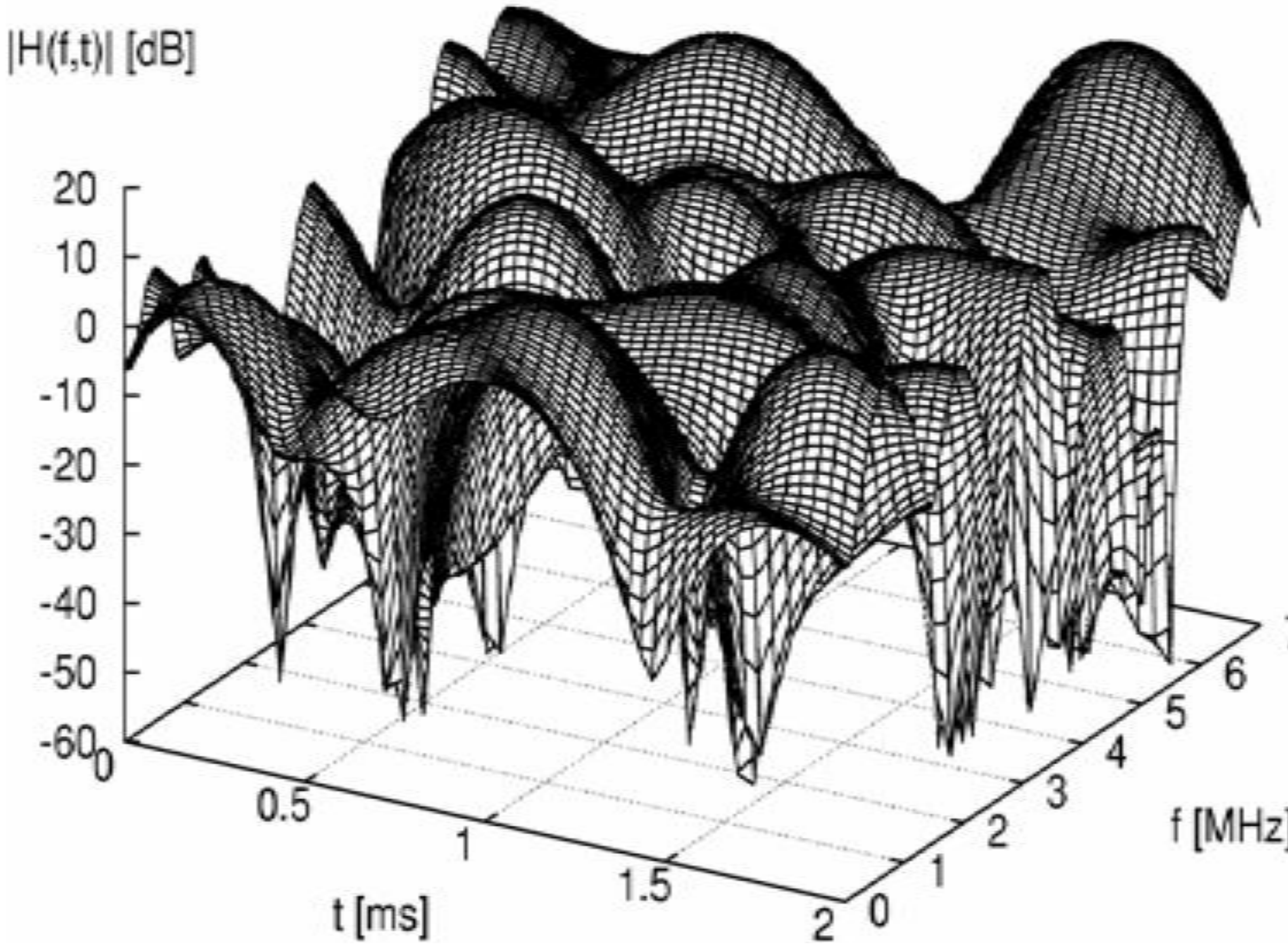

|H(f,t)| [dB]
20
10
0
-10
-20
-30
-40
-50
-60
0
0.5
1
1.5
2
t [ms]
0
1
2
3
4
5
6
7
f [MHz]

Flat-fading (non-freq. Selective)

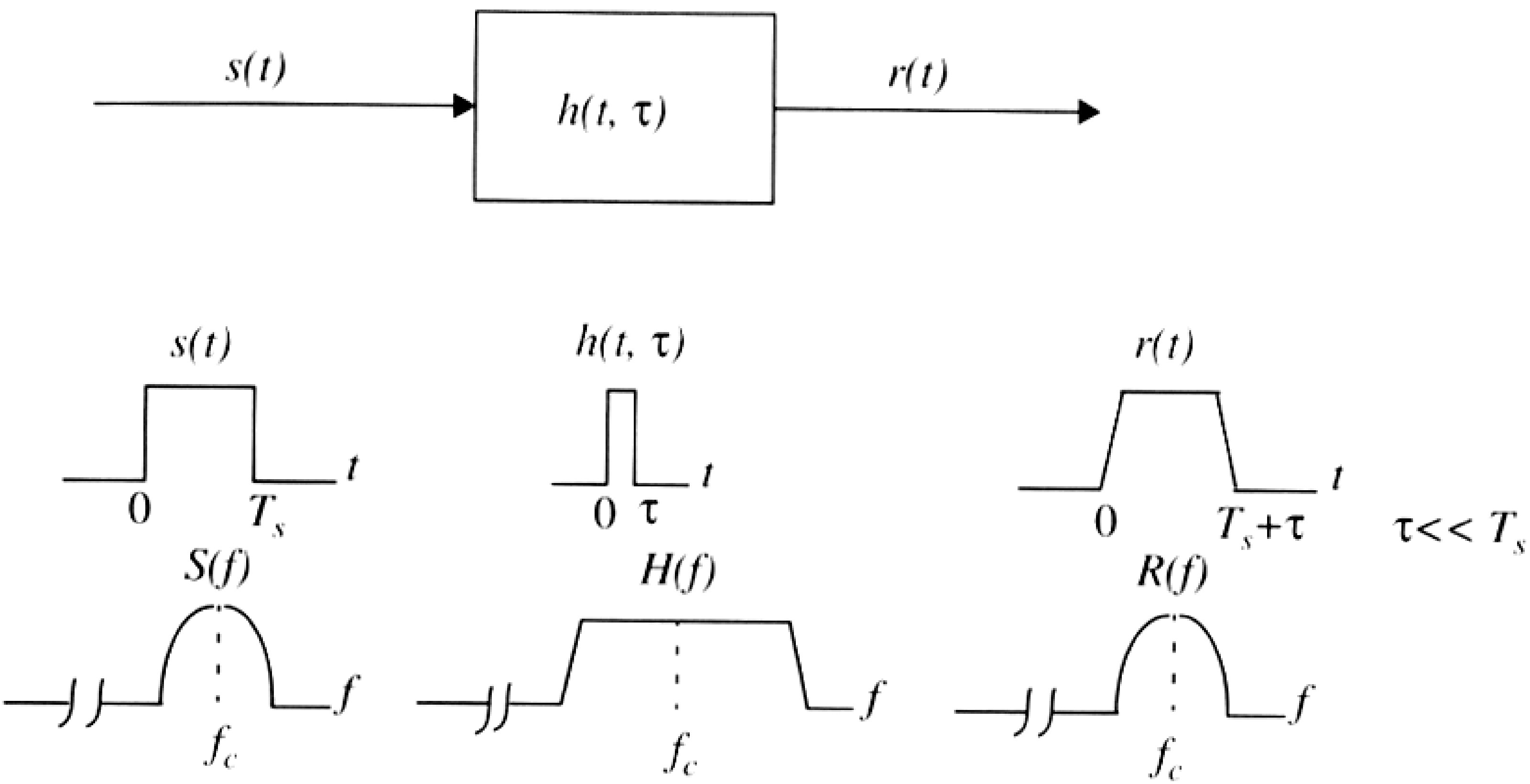

Figure 5.12 Flat fading channel characteristics.

Frequency selective fading

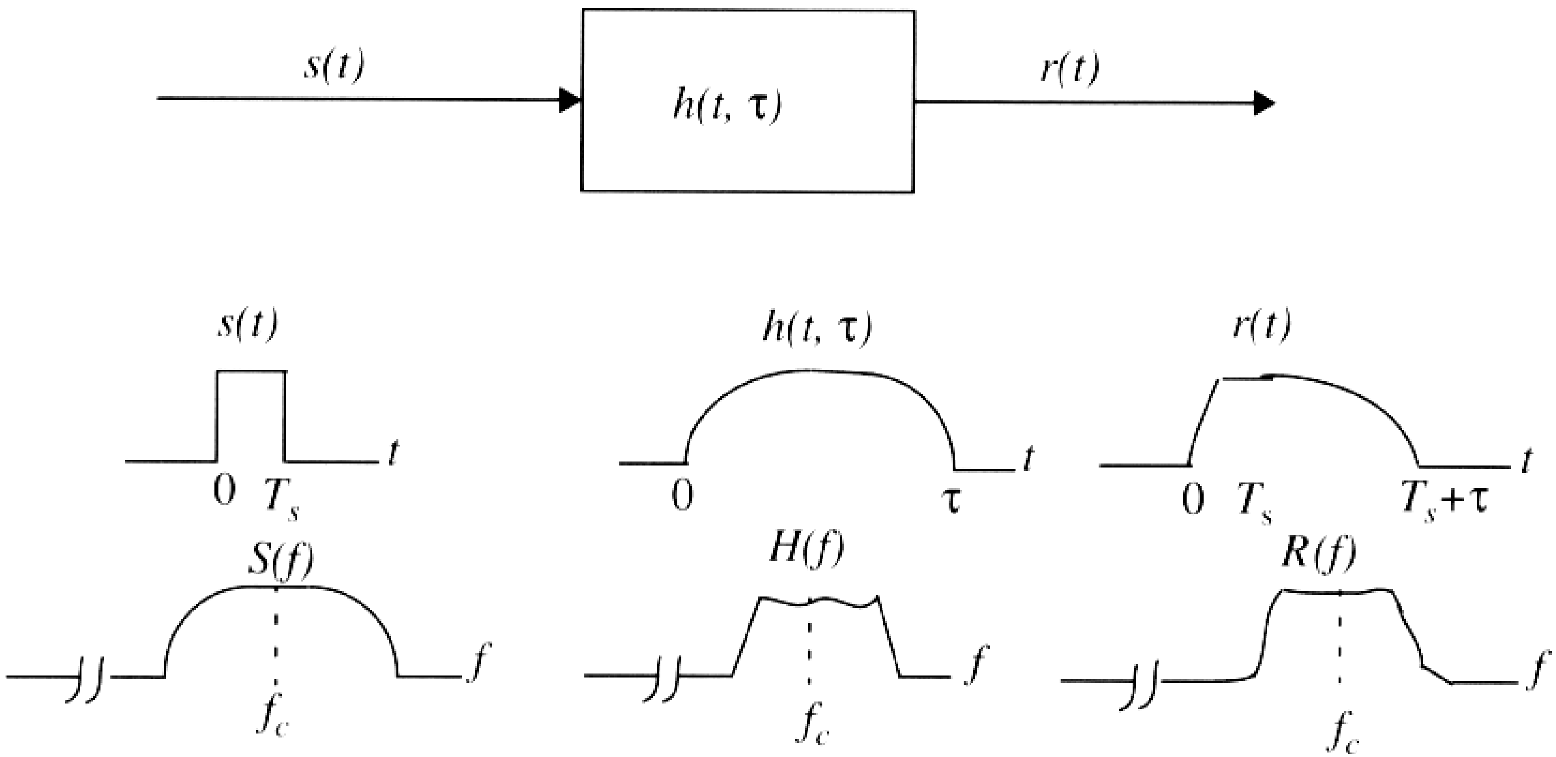

Figure 5.13 Frequency selective fading channel characteristics.

Two independent fading issues

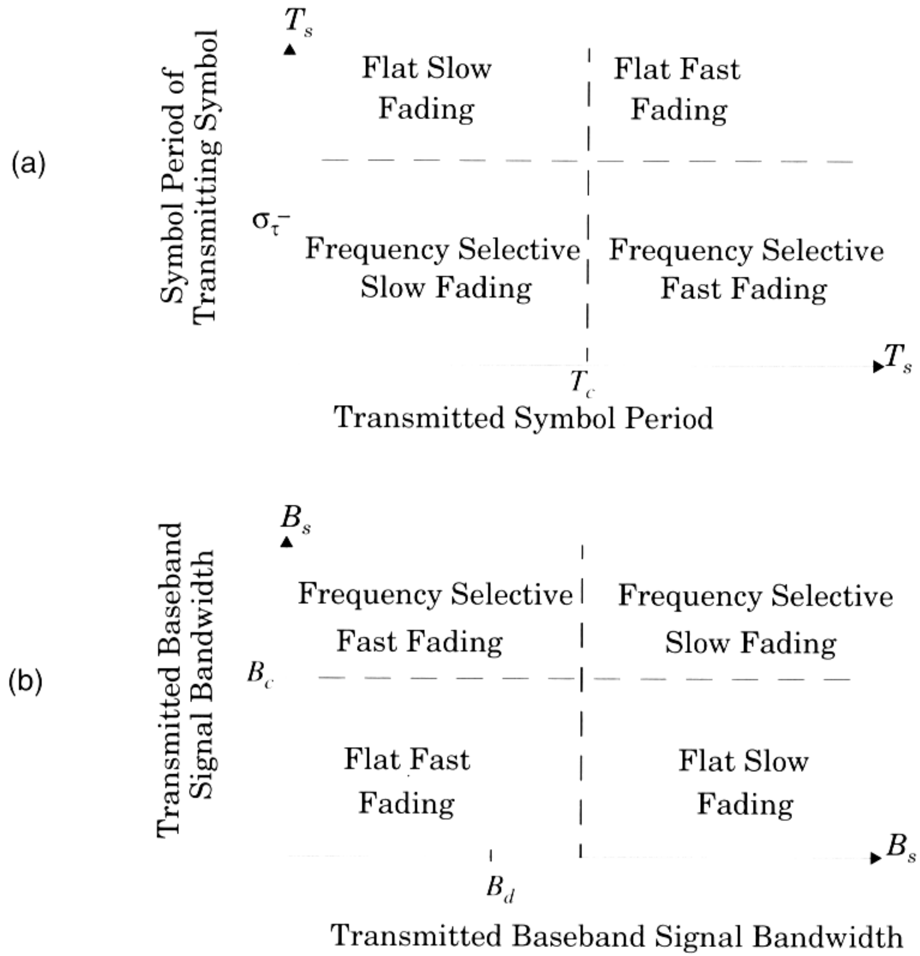

Figure 5.14 Matrix illustrating type of fading experienced by a signal as a function of: (a) symbol period; and (b) baseband signal bandwidth.

Rayleigh fading

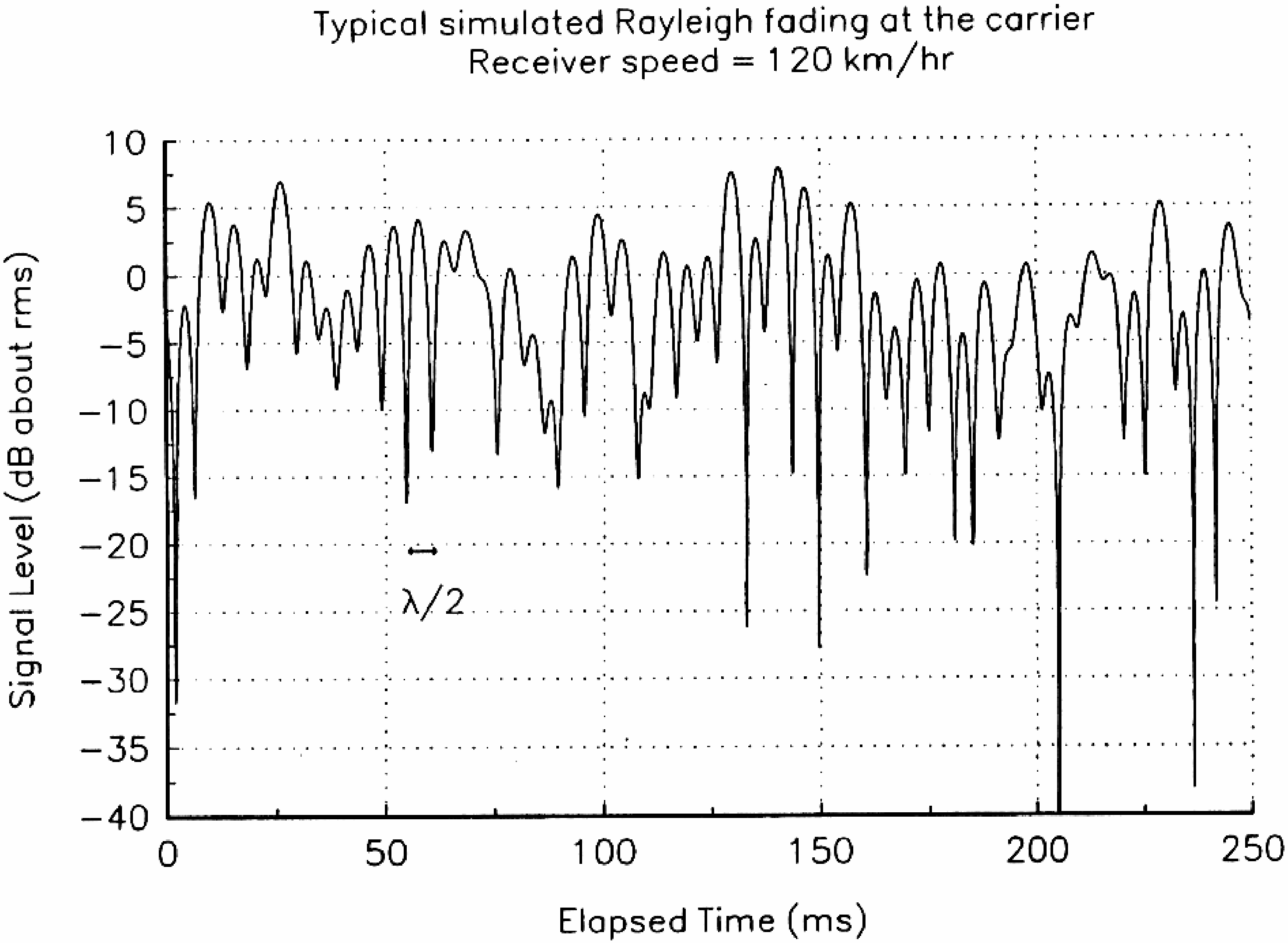

Figure 5.15 A typical Rayleigh fading envelope at 900 MHz [from [Fun93] © IEEE].

Small-scale envelope distributions

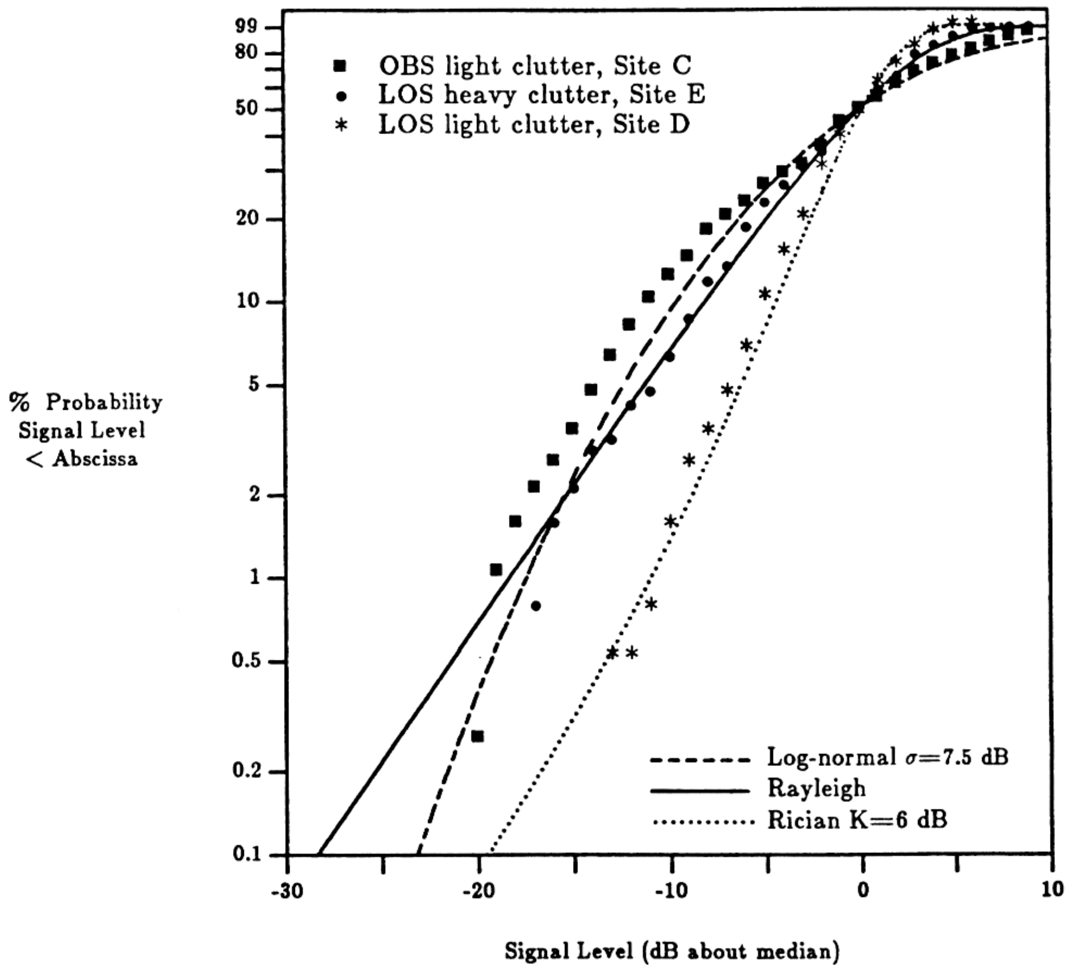

Figure 5.17 Cumulative distribution for three small-scale fading measurements and their fit to Rayleigh, Ricean, and log-normal distributions [from [Rap89] © IEEE].

Ricean and Rayleigh fading distributions

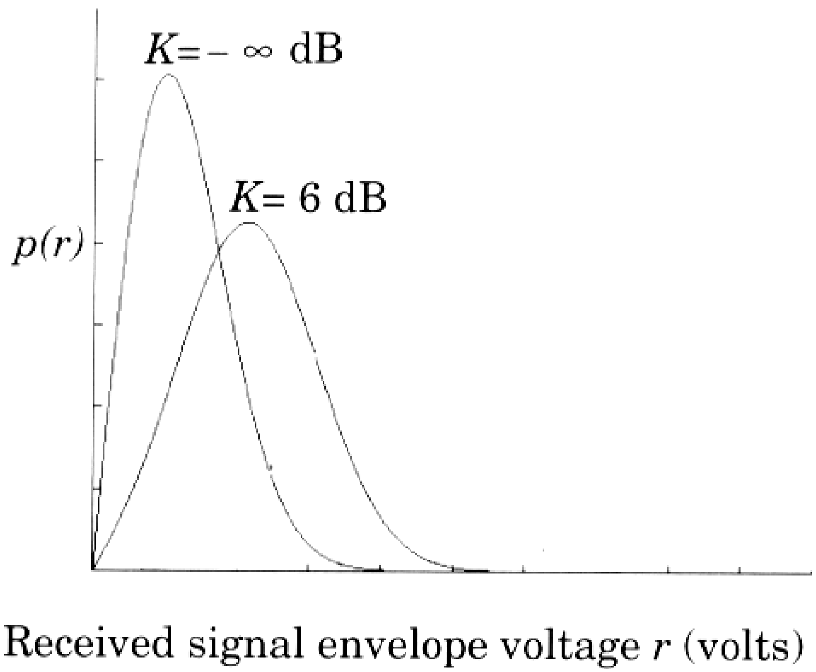

Figure 5.18 Probability density function of Ricean distributions: $K = -\infty$ dB (Rayleigh) and $K = 6$ dB. For K >> 1, the Ricean pdf is approximately Gaussian about the mean.

Small-scale fading mechanism

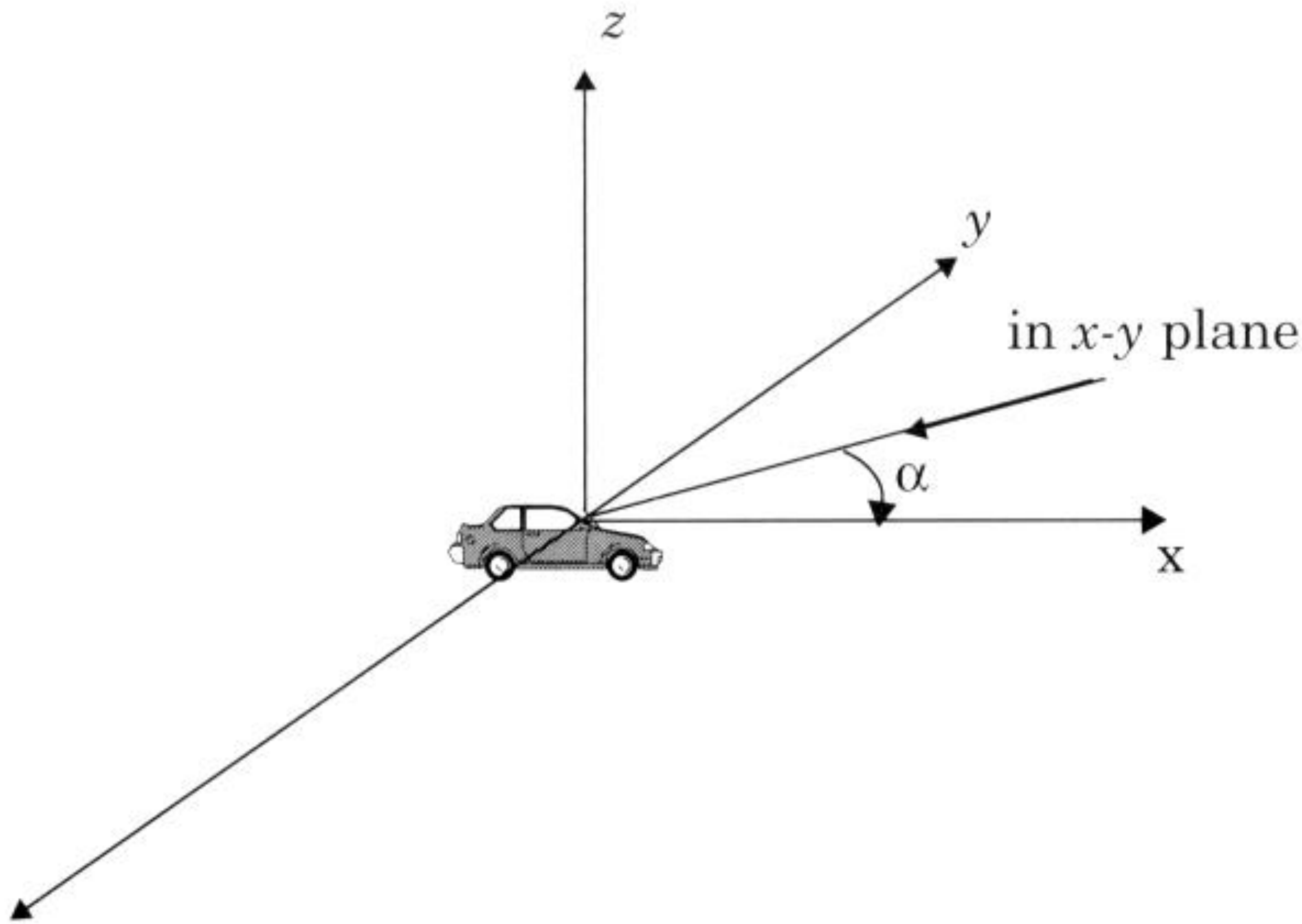

Figure 5.19 Illustrating plane waves arriving at random angles.

Doppler spectrum

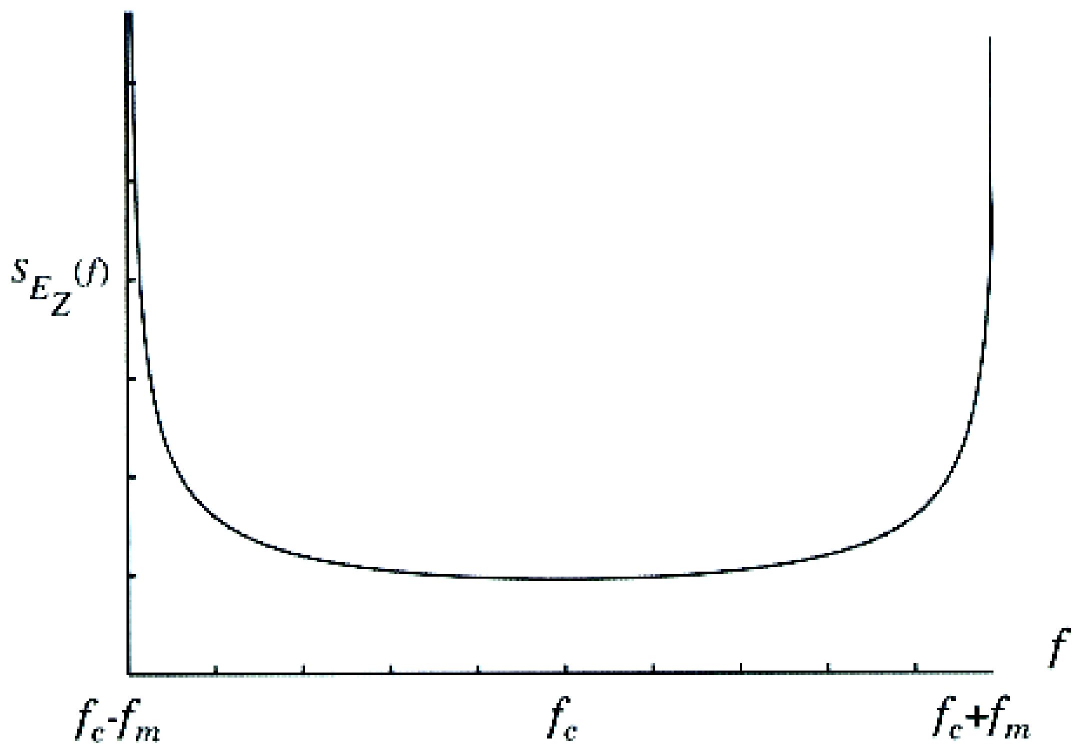

Figure 5.20 Doppler power spectrum for an unmodulated CW carrier [from [Gan72] © IEEE].

Spectrum of Envelope of doppler faded signal

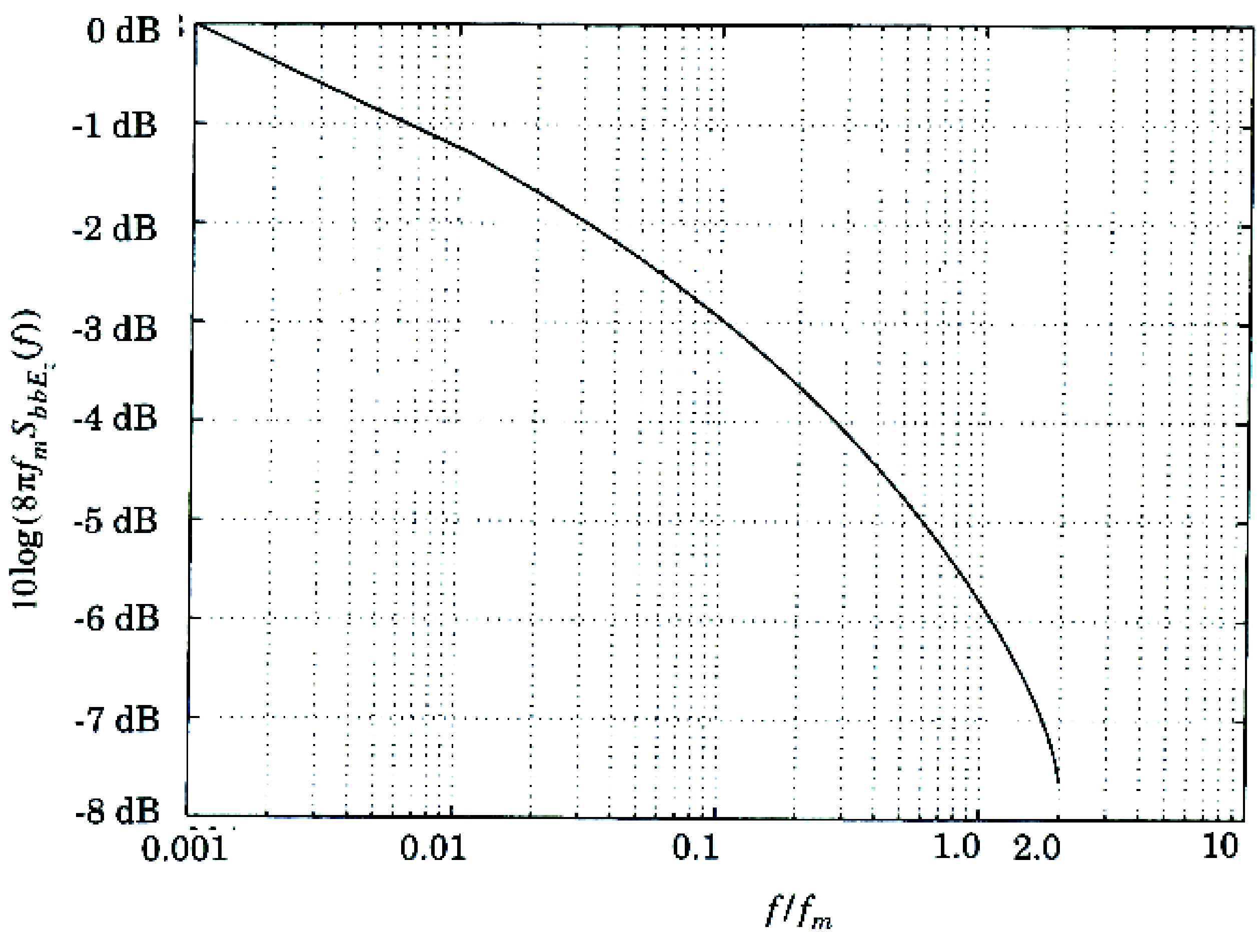

Figure 5.21 Baseband power spectral density of a CW Doppler signal after envelope detection.

Simulating Doppler/Small-scale fading

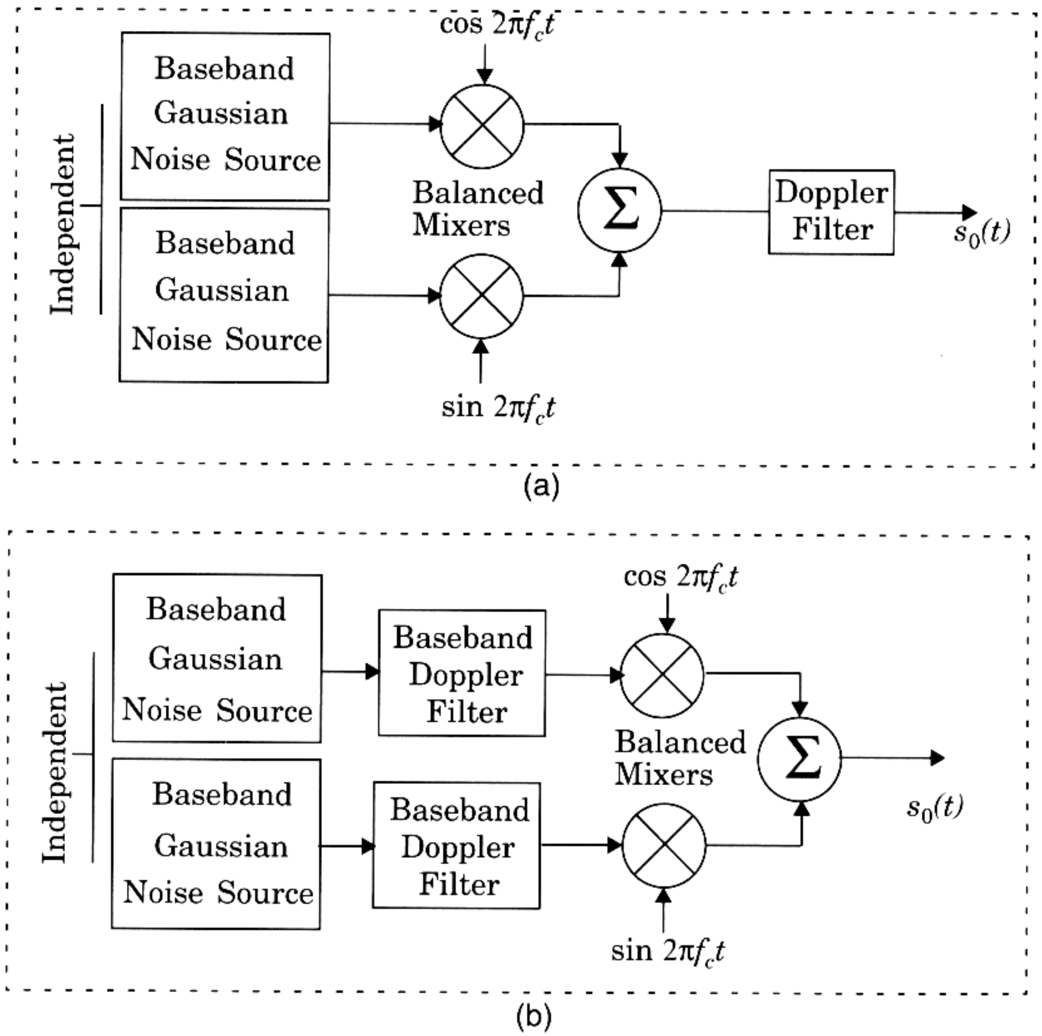

Figure 5.22 Simulator using quadrature amplitude modulation with (a) RF Doppler filter and (b) baseband Doppler filter.

Simulating Doppler fading

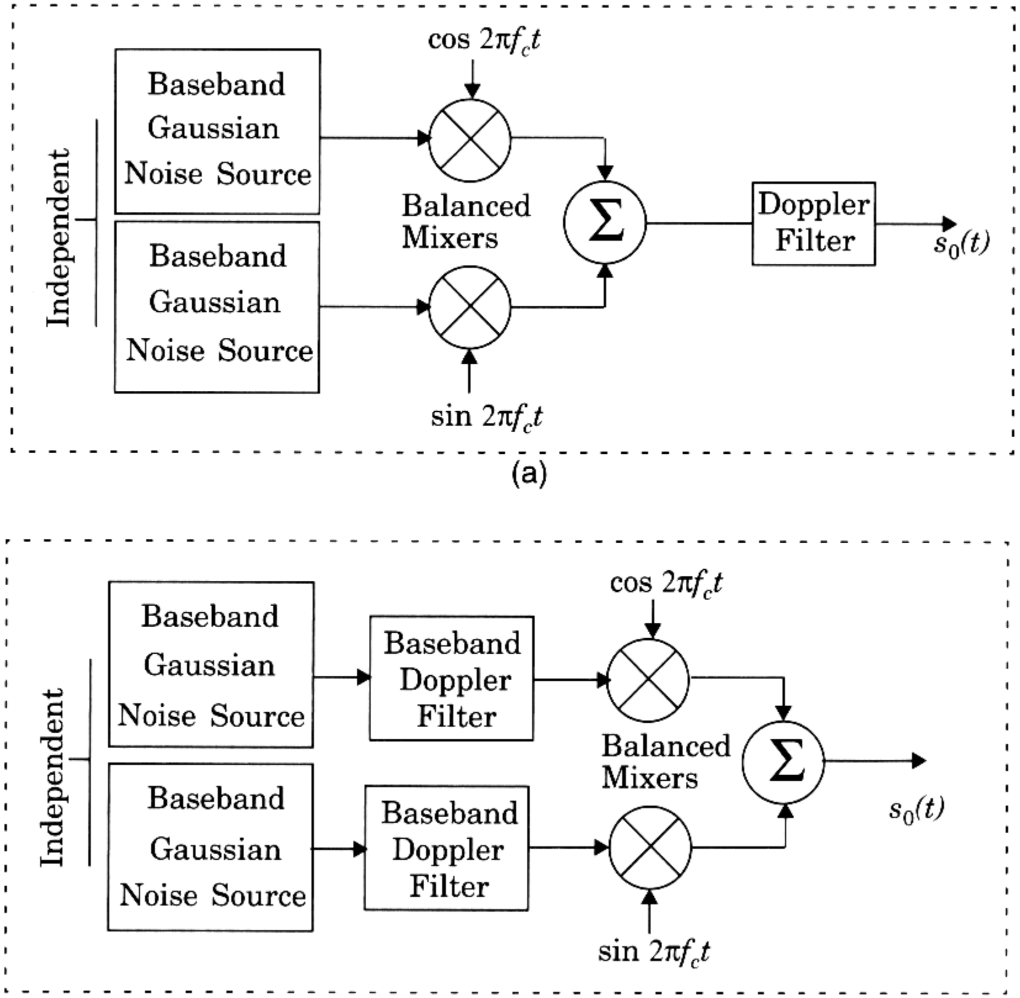

(a)

(b)

Figure 5.23 Simulator using quadrature amplitude modulation with (a) RF Doppler filter and (b) baseband Doppler filter.

Simulating Doppler fading

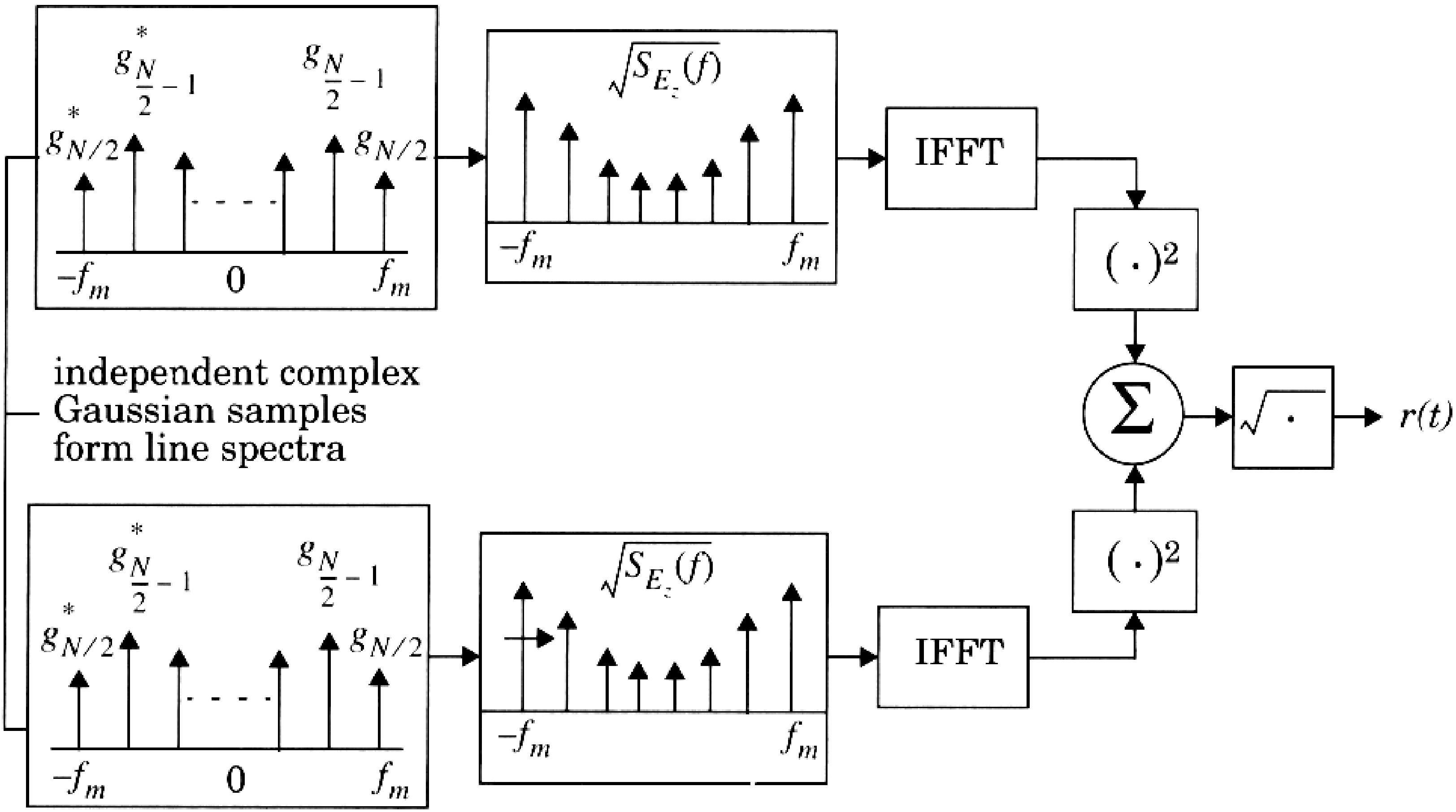

Figure 5.24 Frequency domain implementation of a Rayleigh fading simulator at baseband

Simulating multipath with Doppler-induced Rayleigh fading

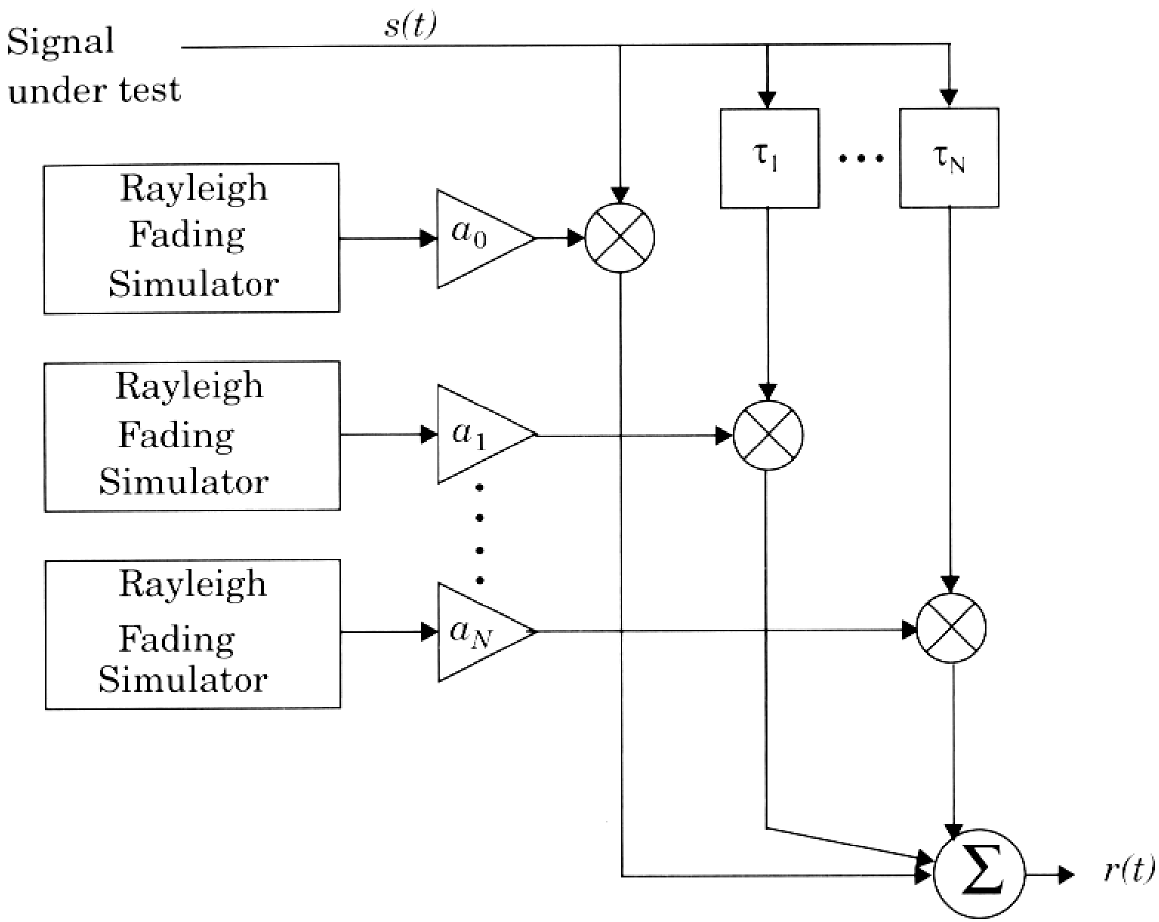

Figure 5.25 A signal may be applied to a Rayleigh fading simulator to determine performance in a wide range of channel conditions. Both flat and frequency selective fading conditions may be simulated, depending on gain and time delay settings.

Simulating 2-ray multipath

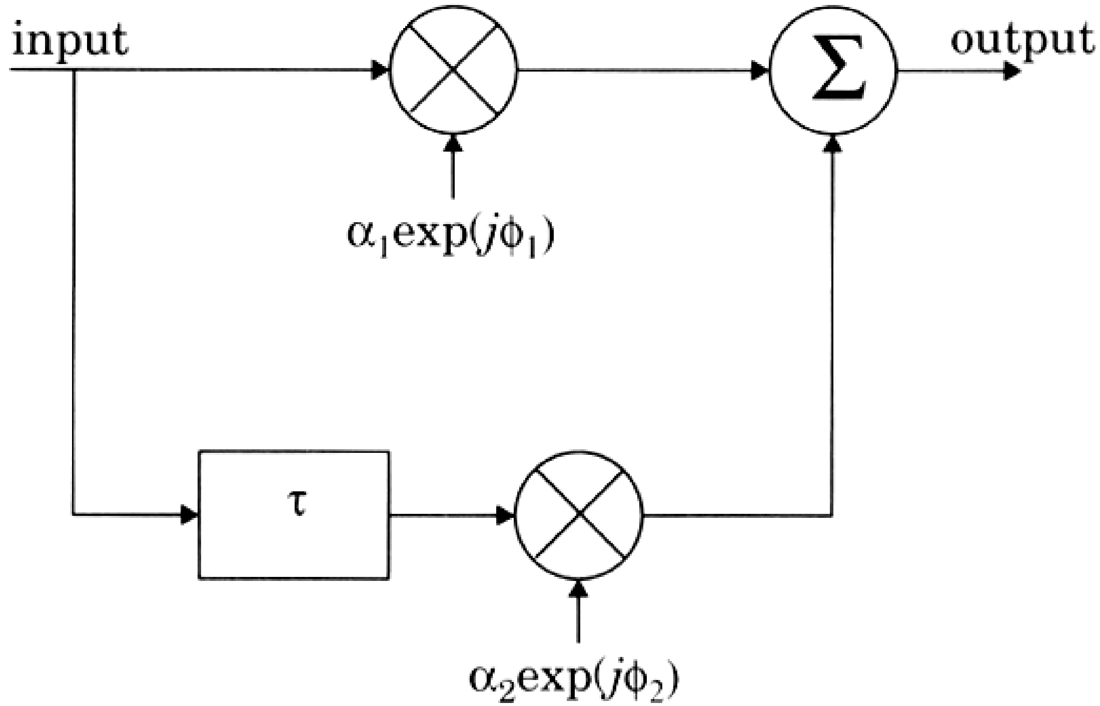

Figure 5.26 Two-ray Rayleigh fading model.

SIRCIM – Simulation of all indoor propagation Characteristics

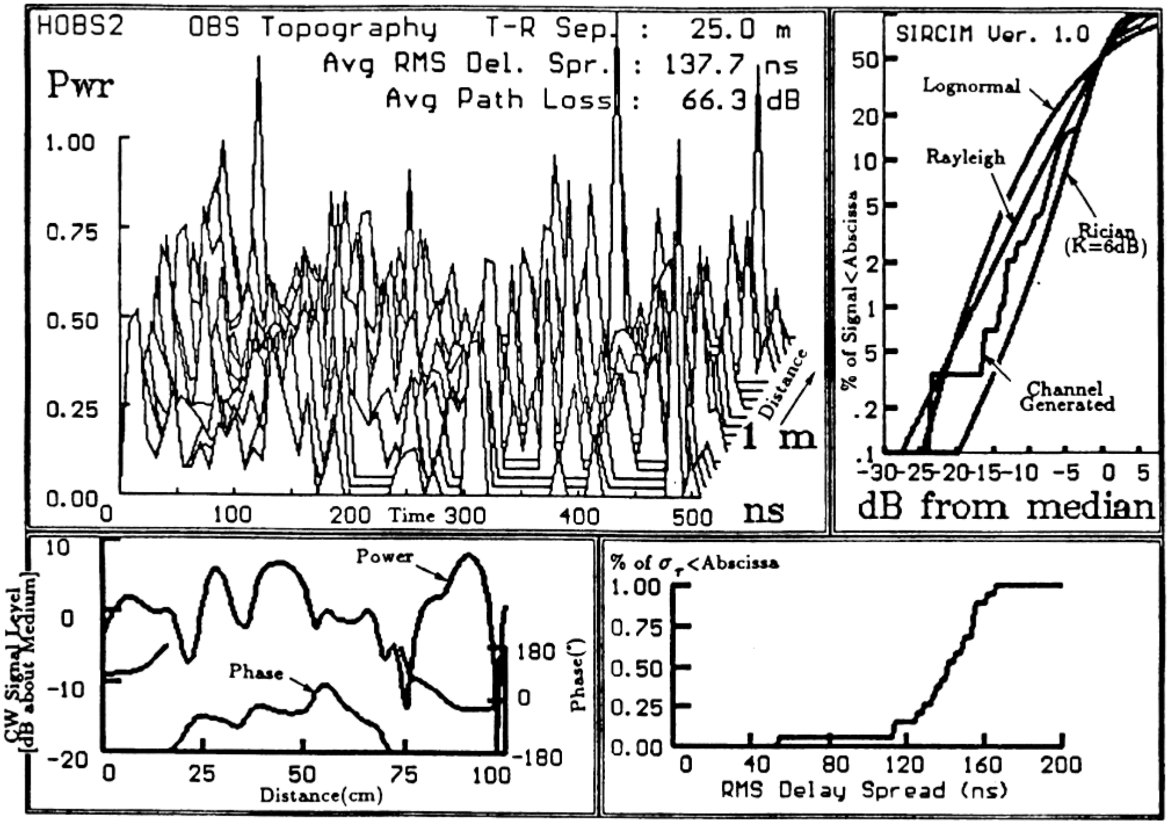

Figure 5.27 Indoor wideband impulse responses simulated by SIRCIM at 1.3 GHz. Also shown are the distributions of the rms delay spread and the narrowband signal power distribution. The channel is simulated as being obstructed in an open-plan building, T–R separation is 25 m. The rms delay spread is 137.7 ns. All multipath components and parameters are stored on disk [from [Rap93a] © IEEE].

SMRCIM – Simulation of all outdoor propagation Characteristics

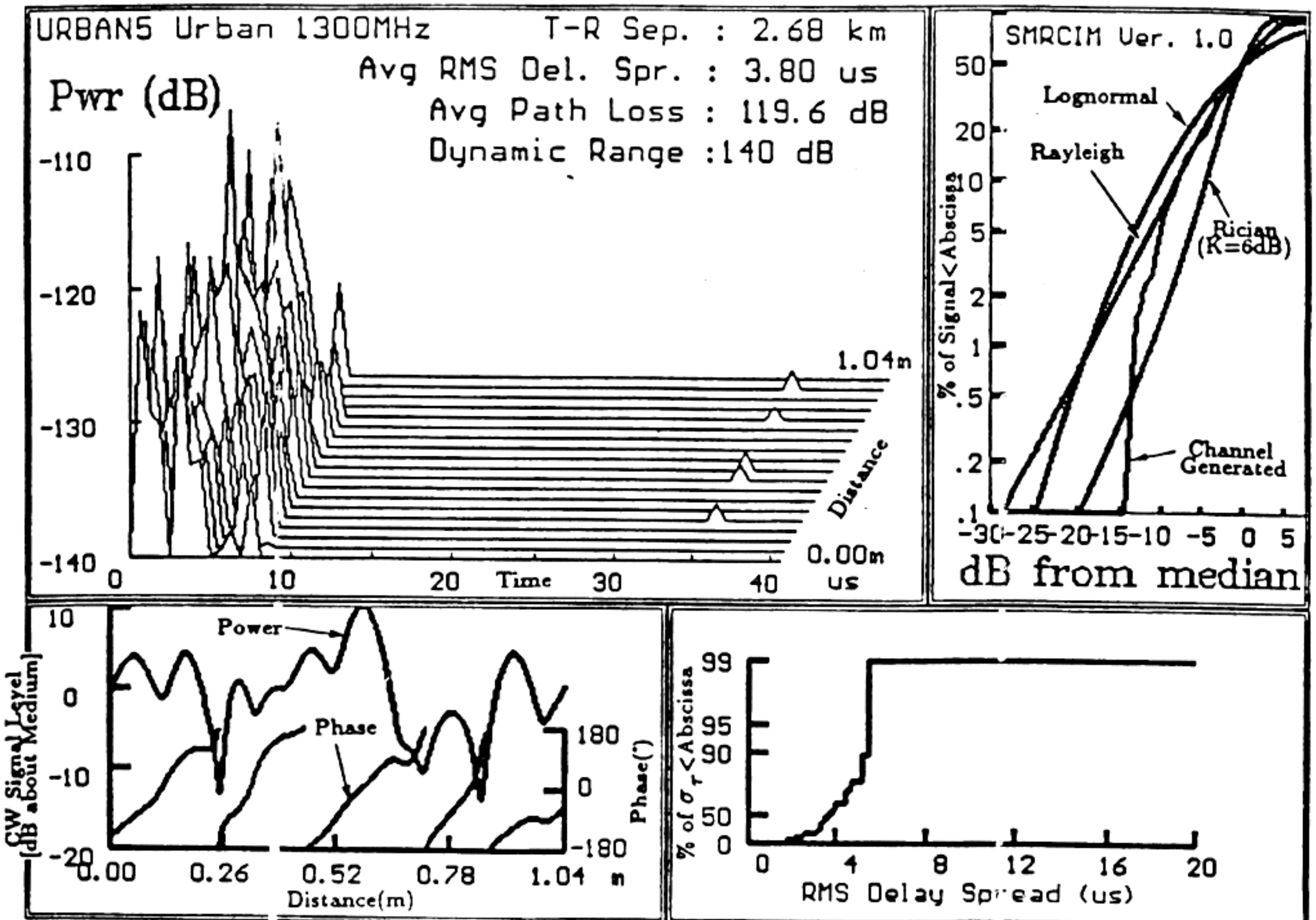

Figure 5.28 Urban wideband impulse responses simulated by SMRCIM at 1.3 GHz. Also shown are the distributions of the rms delay spread and the narrowband fading. T–R separation is 2.68 km. The rms delay spread is 3.8 μs. All multipath components and parameters are saved on disk. [from [Rap93a] © IEEE].

SIRCIM and SMRCIM

- Available from Wireless Valley Communications, Inc.
- Source code in C is available
- www. Wirelessvalley.com

Angular Spread model

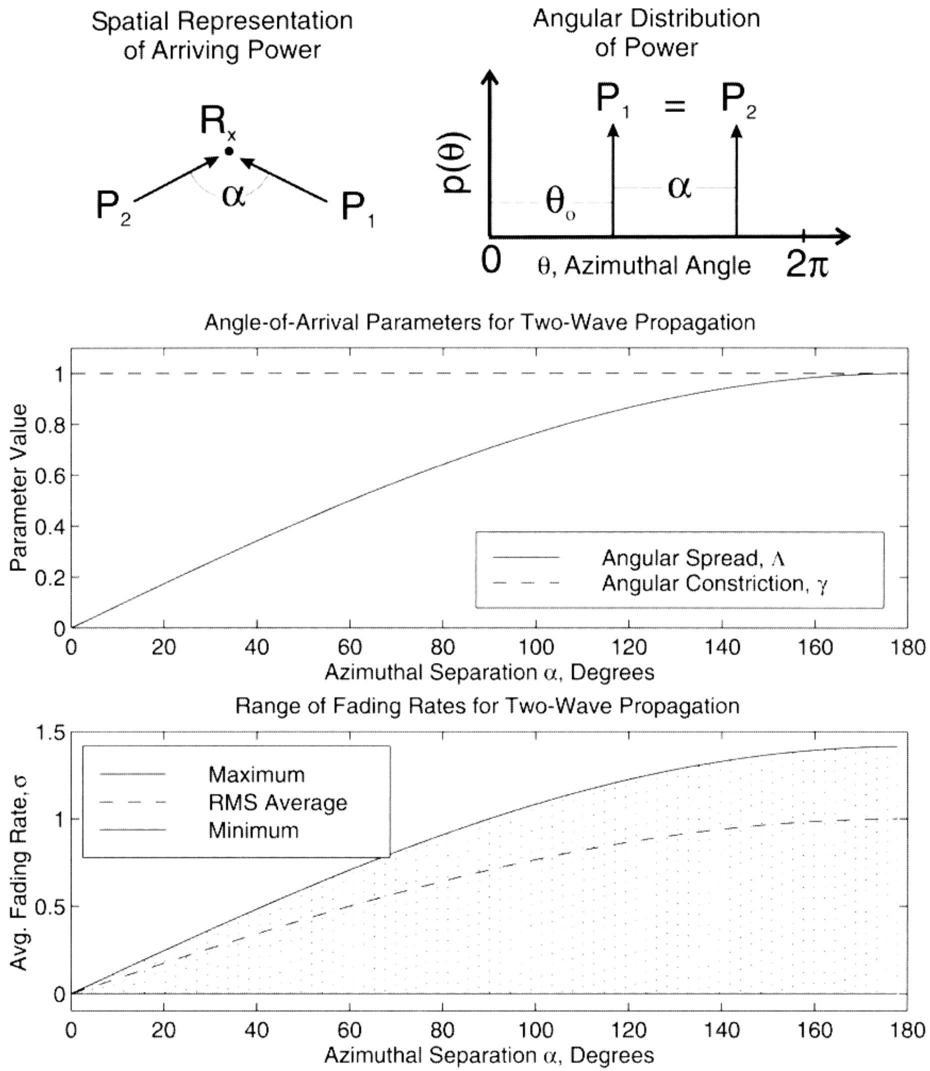

Figure 5.29 Fading properties of two multipath components of equal power [from [Dur00] ©IEEE].

Spatial distribution of Multipath

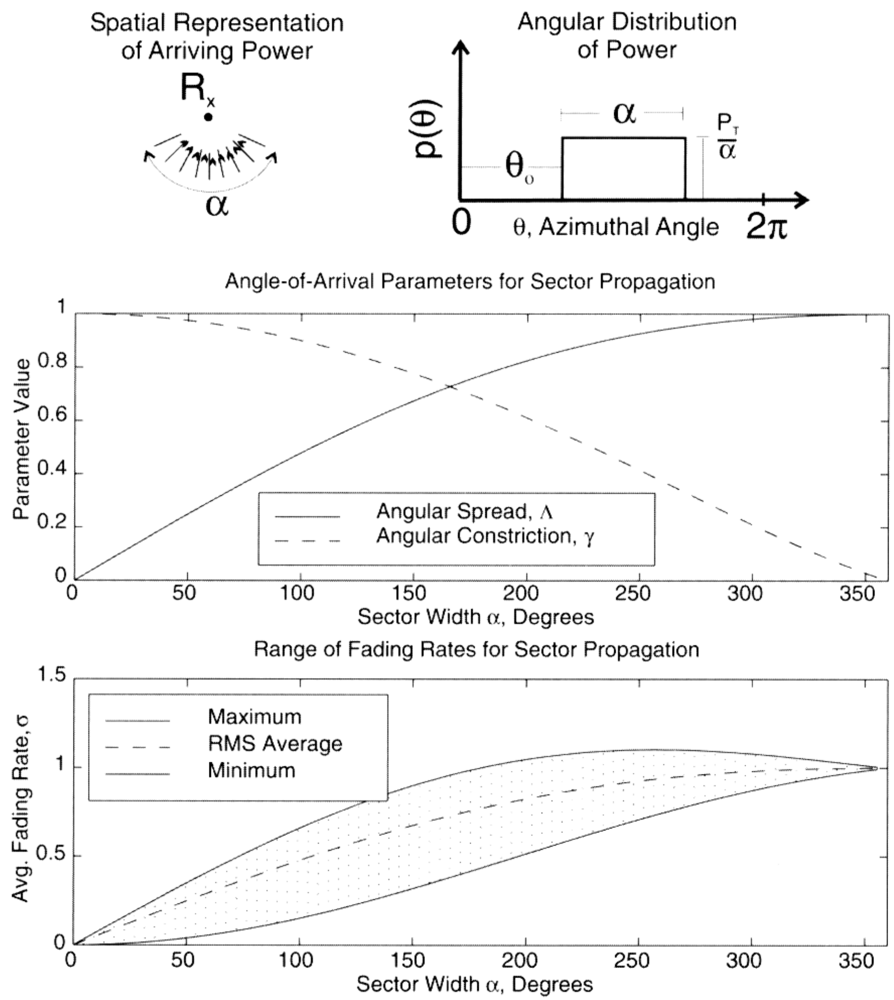

Figure 5.30 Fading properties of a continuous sector of multipath components [from [Dur00] ©IEEE].

Angular Spread key to fading

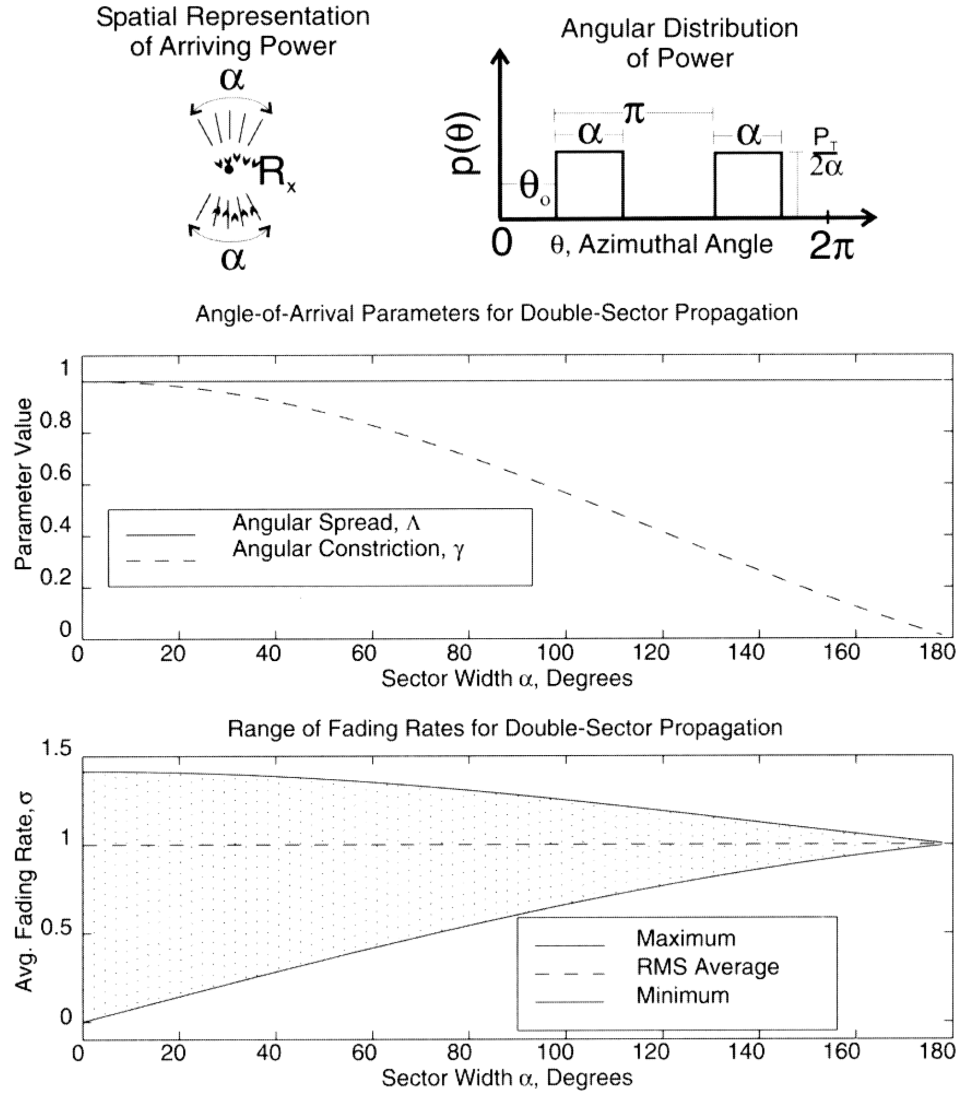

Figure 5.31 Fading properties of double-sectored multipath components [from [Dur00] ©IEEE].

Spatial orientation of multipath impacts the depths of fading

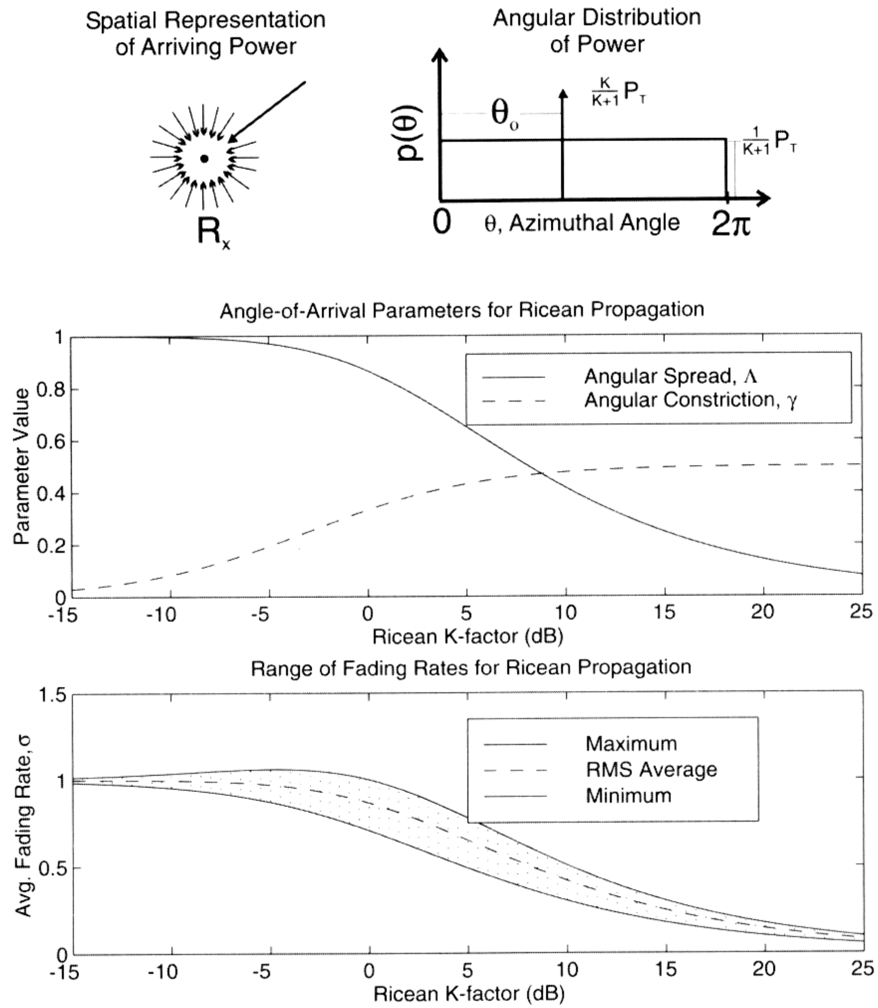

Figure 5.32 Fading properties of Ricean-model multipath components [from [Dur00] ©IEEE].

Angular Distribution of power

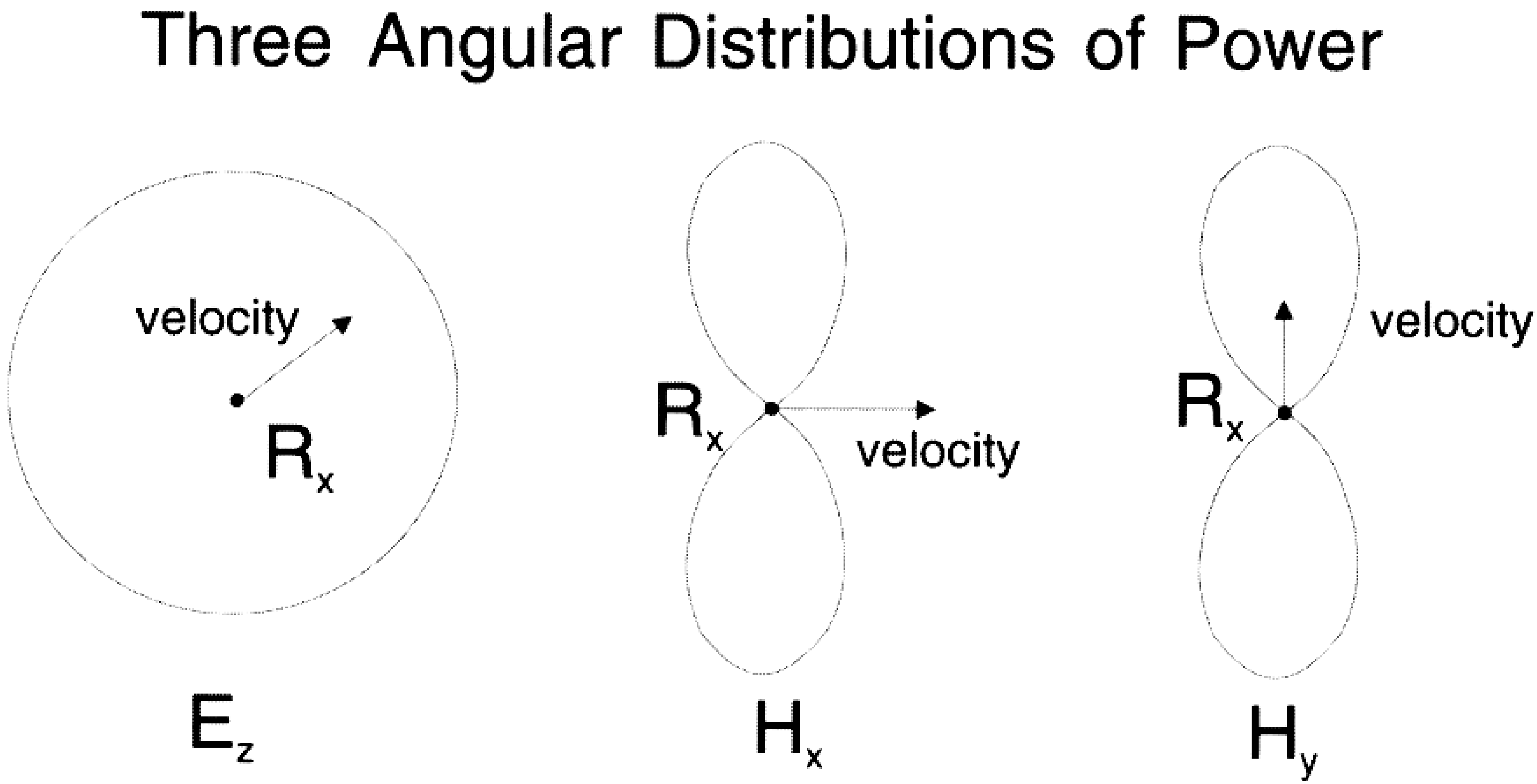

Figure 5.33 Three different multipath-induced mobile-fading scenarios [from [Dur00] ©IEEE].

Angular Spread predicts correlation distances

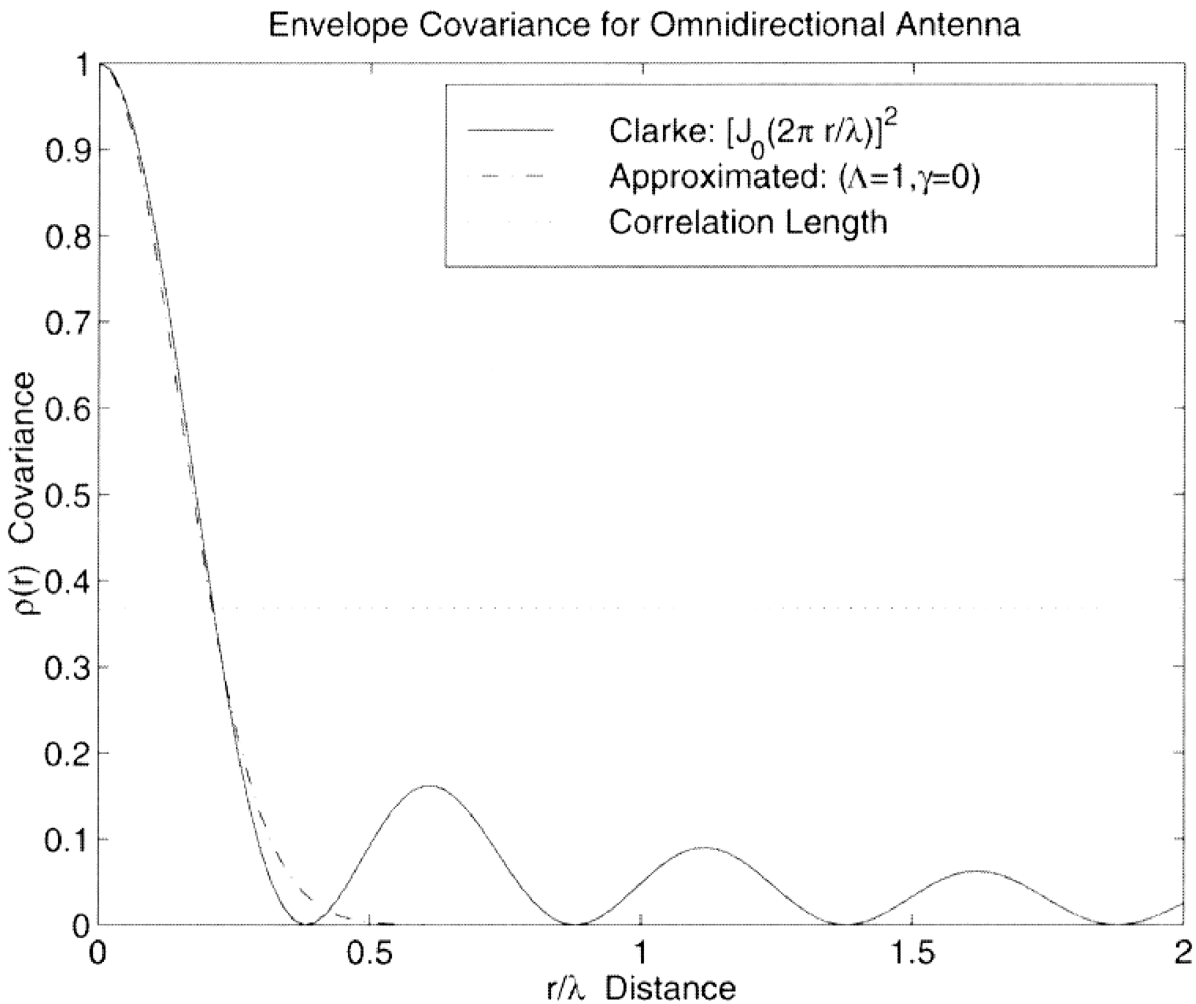

Figure 5.34 Comparison between Clarke theoretical and the shape theory approximation for envelope autocovariance functions for E_z-case [from [Dur00] ©IEEE].

Angular Spread predicts correlation distances

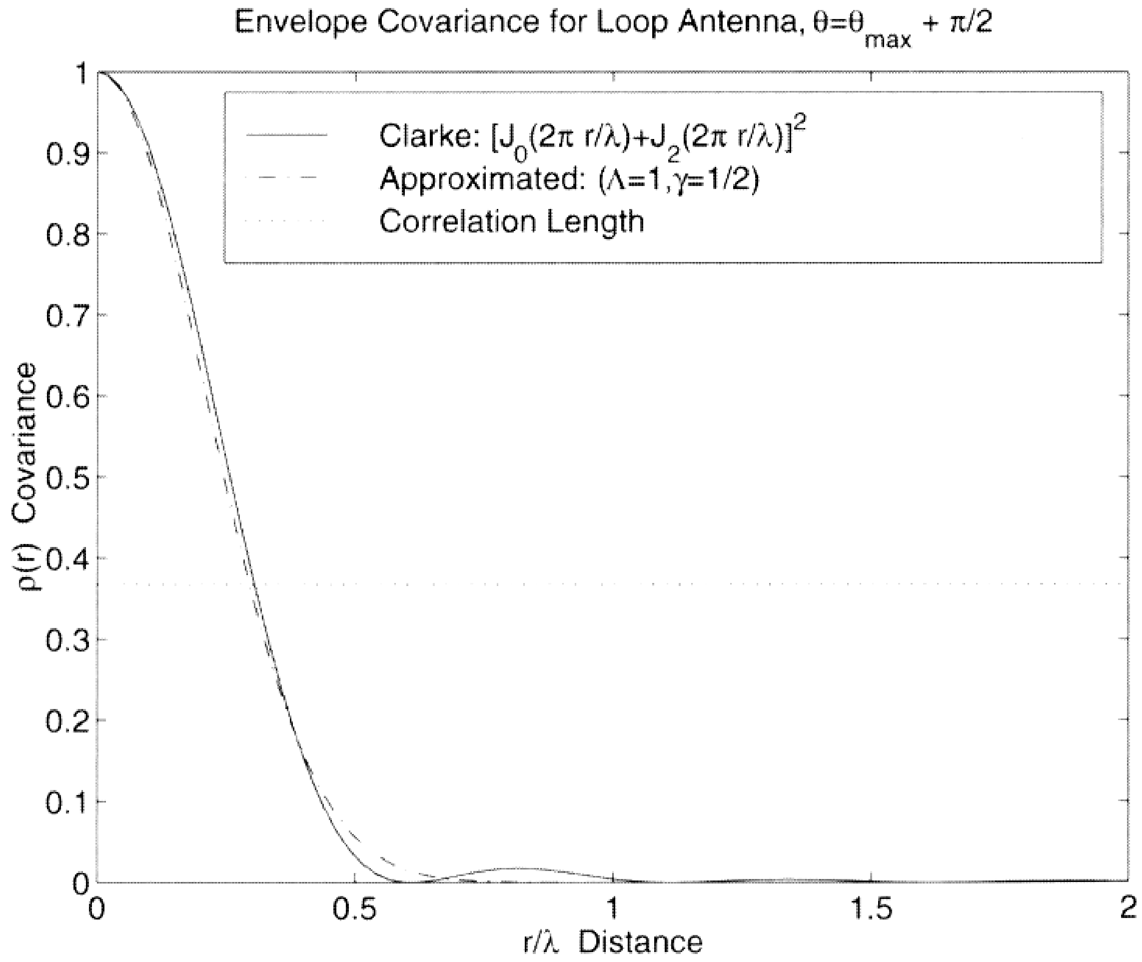

Figure 5.35 Comparison between Clarke theoretical and the shape theory approximation for envelope autocovariance functions for H_x-case [from [Dur00] ©IEEE].